

**Dispersion tensor in stratified porous media**Morteza Dejam<sup>1,\*</sup> and Hassan Hassanzadeh<sup>2,†</sup><sup>1</sup>*Department of Petroleum Engineering, College of Engineering and Applied Science, University of Wyoming, 1000 East University Avenue, Laramie, Wyoming 82071-2000, USA*<sup>2</sup>*Department of Chemical and Petroleum Engineering, Schulich School of Engineering, University of Calgary, 2500 University Drive NW, Calgary, Alberta, Canada T2N 1N4*

(Received 18 January 2022; revised 24 May 2022; accepted 26 May 2022; published 30 June 2022)

Dispersion in porous media is of great importance in many areas of science and engineering. While dispersion in porous media has been generally well discussed in the literature, little work has been done regarding a generalization of Taylor dispersion in stratified media. In this work, we generalized the Taylor dispersion theory and Stokes flow in porous media to derive a reduced-order model for tracer dispersion in stratified porous media. Our findings revealed that for a simple case of two-layer porous media, the hydrodynamic coupling between the two layers leads to the tensorial nature of dispersion and advection. The results showed that the obtained dispersion tensor and advection are not symmetric unless both porous layers have similar thickness, porosity, and molecular diffusion. We found that the main elements of the coefficient of the dispersion tensor remain positive while the off-diagonal elements can take negative values. On the contrary, all elements of the advection matrix may take negative values. On the basis of these observations, we report the manifestation of the dispersion barrier, uphill dispersion and advection, and osmotic dispersion during tracer transport in stratified porous media. In particular, the identified uphill advection reveals that the injected tracer in one layer could be transported countercurrent to the adjacent layer. Furthermore, we have shown that in the limiting case of Darcy flow, the Taylor dispersion is absent, and the tracer mixing between the two layers is restricted to the cross-diffusive flux between them. The results revealed that the field scale mixing may not necessarily originate from the Taylor dispersion and could be due to the modified advection terms and the cross-diffusive flux between the two layers.

DOI: [10.1103/PhysRevE.105.065115](https://doi.org/10.1103/PhysRevE.105.065115)**I. INTRODUCTION**

The longitudinal dispersion coefficient of a tracer matter, or the so-called Taylor dispersion [1], in laminar flow in various geometries is well studied. The Taylor dispersion arises because of the combined effect of shear and transversal diffusion. The transport processes of a chemical species, where Taylor [1] dispersion plays an important role, manifest in various pressure-driven flows, including geophysical flows [2,3], rivers [4], microfluidic devices [5,6], and blood vessels [7]. The tracer transport and dispersion in stratified porous media (i.e., two or more parallel porous layers) find numerous applications in science and engineering, such as enhanced oil recovery [8], geothermal energy extraction [9], geological storage of carbon dioxide [10,11] and hydrogen [12], groundwater hydrology [13], spreading of contaminants in wetlands [14], chemical separation of mixtures in membranes [15], and drug delivery for medical treatments [16]. Taylor dispersion theory has been widely used to obtain the dispersion coefficient of tracer matter for laminar flow in various geometries in open fluids and porous media.

Using the method of moments, Aris [17] developed an expression for dispersion during tracer transport in a gas-

liquid flow within an annular space between two concentric cylinders. This expression includes the effects of the diffusion and advection in the gas, the transfer rate at the interface between gas and liquid, and the diffusion and advection in the liquid [17]. The problem studied by Aris [17] finds interesting applications in transport phenomena. For example, Ng [18] revised this problem using the averaging technique to evaluate the tracer transport in a gas flow within a cylinder conditional on mass transfer and reaction with an immobile liquid on the wall of the cylinder [18].

Using an averaging technique, Wu and Chen [19] generalized the Taylor dispersion theory to obtain a formulation for dispersion during tracer transport through a fully developed flow in a long tube of two zones distinctively packed with porous media. Later, Griffiths *et al.* [20] used asymptotic analysis to derive the dispersion coefficient for solute transport in a thin porous tube, where Stokes and Darcy equations were coupled through the Beavers and Joseph condition at the interface [21]. Thereafter, Ling *et al.* [22,23] focused on tracer transport in a coupled system composed of a channel and a permeable porous medium, where the flow in these two media is governed by Stokes and Darcy-Brinkman equations, respectively. Using the perturbation theory along with asymptotic analysis [22] and integral transforms [23] led to an analytical expression relating the dispersion coefficient with the porosity and permeability of channel walls [22,23]. The authors [22,23] compared their results with the proposed model by

\*mdejam@uwyo.edu

†hhassanz@ucalgary.ca

Dejam *et al.* [24] for tracer transport in a fracture surrounded by an impermeable porous medium. Subsequently, Kou and Dejam [25] extended the study performed by Ling *et al.* [22] to address the dispersion due to combined pressure-driven and electro-osmotic flows in a channel surrounded by a permeable porous medium.

Recently, Dejam and Hassanzadeh [26] generalized Taylor's approach on the dispersion phenomenon to model tracer transport in a two-phase laminar flow of immiscible fluids in a slit using Reynolds decomposition and averaging techniques. It is shown that the dispersion is tensorial due to the presence of an interface between the two fluids [26]. Other efforts in obtaining longitudinal and transverse dispersion in porous media have been reported by Emami Meybodi and Hassanzadeh [11,27] where Taylor's dispersion has been adopted to derive analytical expressions for hydrodynamic dispersion in steady and transient buoyancy-driven flows with applications for solutal convection and geological storage of CO<sub>2</sub> in deep saline aquifers. However, the extension of this theory to stratified porous media has remained a challenge.

In this study, we generalize the Taylor dispersion theory to tracer transport in stratified porous media. First, we derive the velocity distributions in a two-layer stratified porous medium using the fully developed Stokes flow. This is achieved by coupling the Darcy-Brinkman equations in the lower and upper porous media subject to the continuity of velocity and shear stress at the interface between two porous media and the no-slip condition at the top and bottom boundaries. Next, we model the tracer transport in the stratified porous media by coupling the advection-diffusion equations in the lower and upper strata subject to the continuity of tracer concentration and mass flux at the interface between two porous layers and no-mass flux at the top and bottom boundaries. Then, the generalized reduced-order model of advection-dispersion tracer transport in the stratified porous media is derived using the Reynolds decomposition and averaging techniques, followed by an evaluation of the resultant dispersion tensor. Finally, the reduced-order model is solved numerically using a fully implicit finite difference (FD) approach to study the dispersion of tracer matter in stratified porous media. The analysis of the dispersion and advection fluxes of an injected tracer along the stratified porous media allowed us to identify unique transport mechanisms.

The rest of this paper is organized as follows. First, the physical model, assumptions, and mathematical formulation are developed. The Results and Discussion are then presented, followed by the Summary and Conclusions.

## II. PHYSICAL MODEL, ASSUMPTIONS, AND MATHEMATICAL FORMULATION

### A. Physical model and assumptions

Figure 1 shows a schematic of the problem. The system is composed of two infinitely long strata, where porous layer 1 is the lower stratum of thickness  $H_1$ , and porous layer 2 is the upper stratum of thickness  $H_2$ , and  $H_1 + H_2 = H$ . The inlet of the porous layers and the interface between them are the origins of the longitudinal and transversal directions (or the  $\hat{x}$  and  $\hat{z}$  directions), respectively. Therefore, porous

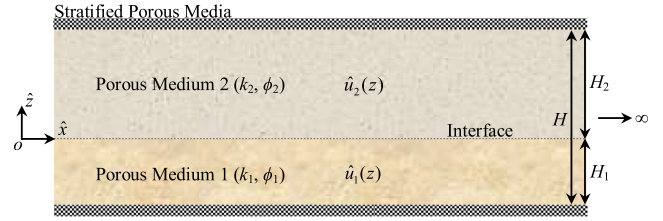


FIG. 1. The physical model for tracer transport in the stratified porous media.

medium 1 occupies the domain  $\hat{z} \in [-H_1, 0]$ , and porous medium 2 occupies the domain  $\hat{z} \in [0, H_2]$ . The physical properties of both strata such as permeability and porosity and the physical properties of fluid, such as density and viscosity, remain constant. The permeability and porosity of porous medium 1 are  $k_1$  and  $\phi_1$ , respectively, and the permeability and porosity of porous medium 2 are  $k_2$  and  $\phi_2$ , respectively. We assume an incompressible single-phase flow of a Newtonian fluid in the longitudinal direction. The fluid flows slowly enough such that no instabilities develop at the interface. The fluid flow in both layers is fully developed laminar, and the velocity distributions are  $\hat{u}_1(z)$  and  $\hat{u}_2(z)$ , respectively. The fluid flow and tracer transport occur in both strata, and they are affected by the momentum and mass transfer across the interface between the two strata.

### B. Derivation of velocity distributions

The fully developed Stokes flow in the stratified porous media can be described by coupling the Darcy-Brinkman equations, which are the second-order linear ordinary differential equations, in the lower and upper strata in nondimensional form as follows:

$$\text{Da}_1 \frac{d^2 u_1}{dz^2} - u_1 + 1 = 0, \quad z \in (-h_1, 0), \quad (1)$$

$$\text{Da}_2 \frac{d^2 u_2}{dz^2} - u_2 + 1 = 0, \quad z \in (0, h_2), \quad (2)$$

where  $u_1 = \hat{u}_1 / -[(k_1/\mu)(d\hat{p}/d\hat{x})]$ ,  $u_2 = \hat{u}_2 / -[(k_2/\mu)(d\hat{p}/d\hat{x})]$ ,  $z = \hat{z}/H$ ,  $\text{Da}_1 = (\mu_{e1}/\mu)(k_1/H^2)$ ,  $\text{Da}_2 = (\mu_{e2}/\mu)(k_2/H^2)$ ,  $h_1 = H_1/H$ ,  $h_2 = H_2/H$ , and  $h_1 + h_2 = 1$ , in which  $\hat{u}_1$  and  $\hat{u}_2$  are the velocities in porous layers 1 and 2, respectively,  $u_1$  and  $u_2$  are the nondimensional velocities in porous layers 1 and 2, respectively,  $\mu$  is the fluid viscosity,  $\mu_{e1}$  and  $\mu_{e2}$  are the effective viscosities in porous layers 1 and 2, respectively,  $\hat{p}$  is the pressure,  $d\hat{p}/d\hat{x}$  is the pressure gradient (which is constant and drives the flow in the longitudinal direction),  $z$  is the nondimensional transversal coordinate,  $\text{Da}_1$  and  $\text{Da}_2$  are the Darcy numbers in porous layers 1 and 2, respectively, and  $h_1$  and  $h_2$  are the nondimensional thicknesses of strata 1 and 2, respectively.

It is noted that the Darcy numbers in layers 1 and 2,  $\text{Da}_1$  and  $\text{Da}_2$ , are both defined based on the thickness of stratified porous media,  $H = H_1 + H_2$ . We also define Darcy numbers in strata 1 and 2 based on the thickness of individual porous layers,  $H_1$  and  $H_2$ . The relationships

between the defined Darcy numbers in porous layers 1 and 2 based on  $H$  ( $\text{Da}_1$  and  $\text{Da}_2$ ) and those defined based on the thickness of individual porous layers ( $\text{Da}_1^*$  and  $\text{Da}_2^*$ ) can be derived as  $\text{Da}_1 = \text{Da}_1^*/[1 + (h_2/h_1)]^2$  and  $\text{Da}_2 = \text{Da}_2^*/[1 + (h_1/h_2)]^2$ , where  $\text{Da}_1^* = (\mu_{e1}/\mu)/(k_1/H_1^2)$  and  $\text{Da}_2^* = (\mu_{e2}/\mu)/(k_2/H_2^2)$ .  $\text{Da}_{1/2}^* = \text{Da}_1^*/\text{Da}_2^*$  is the ratio of the Darcy number in porous layer 1 to porous layer 2 (or simply the Darcy number ratio).

Equations (1) and (2) are subjected to the no-slip condition at the bottom of the porous medium 1 ( $z = -h_1$ ), the continuity of velocity and shear stress at the interface between two porous media ( $z = 0$ ), and the no-slip condition at the top of porous medium 1 ( $z = h_2$ ), as described by

$$u_1|_{z=-h_1} = 0, \quad (3)$$

$$\text{Da}_{1/2} u_1|_{z=0} = u_2|_{z=0}, \quad (4)$$

$$\text{Da}_{1/2} \frac{du_1}{dz} \Big|_{z=0} = \frac{du_2}{dz} \Big|_{z=0}, \quad (5)$$

$$u_2|_{z=h_2} = 0. \quad (6)$$

where  $\text{Da}_{1/2} = \text{Da}_1/\text{Da}_2$  is the ratio of the Darcy number in layer 1 based on  $H$  to the Darcy number in layer 2 based on  $H$ . It is worth noting that  $\text{Da}_{1/2} = (k_1/k_2)(\mu_{e1}/\mu_{e2}) = k_{1/2}\mu_{e1/2}$  where  $k_{1/2}$  is the ratio of the permeability in porous medium 1 to the permeability in porous medium 2 (or simply the permeability ratio) and  $\mu_{e1/2}$  is the ratio of the effective viscosity in porous medium 1 to the effective viscosity in porous medium 2 (or simply the viscosity ratio).

The following analytical solutions for the nondimensional velocity distributions in the stratified porous media can be derived by solving Eqs. (1) and (2) subject to Eqs. (3)–(6):

$$u_1(z) = A_1 \cosh(\eta_1 z) + B_1 \sinh(\eta_1 z) + 1, \quad z \in [-h_1, 0], \quad (7)$$

$$u_2(z) = A_2 \cosh(\eta_2 z) + B_2 \sinh(\eta_2 z) + 1, \quad z \in [0, h_2], \quad (8)$$

where  $\eta_1 = \sqrt{1/\text{Da}_1}$ ,  $\eta_2 = \sqrt{1/\text{Da}_2}$ , and the constants  $A_1$ ,  $A_2$ ,  $B_1$ , and  $B_2$  are defined, respectively, as follows:

$$A_1 = B_1 \tanh \lambda_1 - \text{sech} \lambda_1, \quad (9)$$

$$A_2 = -B_2 \tanh \lambda_2 - \text{sech} \lambda_2, \quad (10)$$

$$B_1 = \frac{\text{Da}_{1/2} [\text{sech} \lambda_1 - 1] + 1 - \text{sech} \lambda_2}{\text{Da}_{1/2} \tanh \lambda_1 + \sqrt{\text{Da}_{1/2}} \tanh \lambda_2}, \quad (11)$$

$$B_2 = \sqrt{\text{Da}_{1/2}} B_1, \quad (12)$$

where  $\lambda_1 = \eta_1 h_1 = H_1/\sqrt{k_1}$  and  $\lambda_2 = \eta_2 h_2 = H_2/\sqrt{k_2}$ .

### C. Governing equations for advection-diffusion tracer transport

The tracer transport in the stratified porous media can be described by coupling the advection-diffusion equations, which are the second-order linear partial differential equa-

tions, in the lower and upper strata in nondimensional form as follows:

$$\frac{\partial c_1}{\partial t} + \text{Pe}_1 u_1 \frac{\partial c_1}{\partial x} = \frac{\partial^2 c_1}{\partial x^2} + \frac{\partial^2 c_1}{\partial z^2},$$

$$x \in (0, \infty), \quad z \in (-h_1, 0), \quad t > 0, \quad (13)$$

$$D_{1/2} \frac{\partial c_2}{\partial t} + \text{Pe}_2 u_2 \frac{\partial c_2}{\partial x} = \frac{\partial^2 c_2}{\partial x^2} + \frac{\partial^2 c_2}{\partial z^2},$$

$$x \in (0, \infty), \quad z \in (0, h_2), \quad t > 0, \quad (14)$$

where  $c_1 = \hat{c}_1/c^*$ ,  $c_2 = \hat{c}_2/c^*$ ,  $x = \hat{x}/H$ ,  $t = D_1 \hat{t}/H^2$ ,  $D_{1/2} = D_1/D_2$ ,  $\text{Pe}_1 = -[(k_1/\mu)(d\hat{p}/d\hat{x})]H/D_1\phi_1$ , and  $\text{Pe}_2 = -[(k_2/\mu)(d\hat{p}/d\hat{x})]H/D_2\phi_2$ , in which  $\hat{c}_1$  and  $\hat{c}_2$  are the tracer concentrations in layers 1 and 2, respectively,  $c_1$  and  $c_2$  are the nondimensional tracer concentrations in strata 1 and 2, respectively,  $c^*$  is the reference tracer concentration,  $x$  is the nondimensional longitudinal coordinate,  $\hat{t}$  is the time,  $t$  is the nondimensional time,  $D_1$  and  $D_2$  are the effective molecular diffusion coefficients in porous media 1 and 2, respectively,  $D_{1/2}$  is the ratio of the effective molecular diffusion coefficient in porous medium 1 to the effective molecular diffusion coefficient in porous medium 2 (or simply the diffusion coefficient ratio or the diffusivity ratio), and  $\text{Pe}_1$  and  $\text{Pe}_2$  are the Péclet numbers for fluid flows in layers 1 and 2, respectively.

Equations (13) and (14) are subjected to the instantaneous injection of tracer at  $t = 0$  (as a pulse) at the inlet of stratified porous media ( $x = 0$ ), zero tracer concentration at an infinite distance from the inlet ( $x \rightarrow \infty$ ), no-mass flux at the bottom of porous medium 1 ( $z = -h_1$ ), the continuity of tracer concentration and mass flux at the interface between two porous media ( $z = 0$ ), and no-mass flux at the top of porous medium 2 ( $z = h_2$ ), as described by

$$c_1[x \in (0, \infty), z \in (-h_1, 0), t = 0]$$

$$= c_2[x \in (0, \infty), z \in (0, h_2), t = 0] = \delta(x), \quad (15)$$

$$c_1[x \rightarrow \infty, z \in (-h_1, 0), t > 0]$$

$$= c_2[x \rightarrow \infty, z \in (0, h_2), t > 0] = 0, \quad (16)$$

$$\frac{\partial c_1[x \in (0, \infty), z = -h_1, t > 0]}{\partial z} = 0, \quad (17)$$

$$c_1[x \in (0, \infty), z = 0, t > 0] = c_2[x \in (0, \infty), z = 0, t > 0], \quad (18)$$

$$D_{1/2} \phi_{1/2} \frac{\partial c_1[x \in (0, \infty), z = 0, t > 0]}{\partial z}$$

$$= \frac{\partial c_2[x \in (0, \infty), z = 0, t > 0]}{\partial z}, \quad (19)$$

$$\frac{\partial c_2[x \in (0, \infty), z = h_2, t > 0]}{\partial z} = 0, \quad (20)$$

where  $\delta(x) = 0$  when  $x \neq 0$ , and  $\phi_{1/2} = \phi_1/\phi_2$  is the ratio of the porosity in porous medium 1 to the porosity in porous medium 2 (or simply the porosity ratio).

Using the Reynolds decomposition and averaging methods, the reduced-order models for advection-dispersion tracer transport in stratified porous media are derived. The detailed

derivation of model reduction is presented in Appendix A for the sake of brevity.

#### D. Dispersion tensor

The advection-dispersion tracer transport in stratified porous media [Eqs. (A42) and (A43)] can be described in matrix form as follows:

$$\begin{bmatrix} 1 \\ D_{1/2} \end{bmatrix} \frac{\partial [\bar{c}]}{\partial t} + [\mathbf{v}] \frac{\partial [\bar{c}]}{\partial x} = [\mathbf{K}] \frac{\partial^2 [\bar{c}]}{\partial x^2} + (\bar{c}_2 - \bar{c}_1) [\mathbf{J}], \quad (21)$$

where  $[\bar{c}]^T = [\bar{c}_1, \bar{c}_2]$ ,  $[\mathbf{v}]$  is the matrix of coefficients of the advection term,  $[\mathbf{K}]$  is the dispersion tensor, and  $[\mathbf{J}]^T = [\frac{1}{h_1} J_1, -\frac{1}{h_2} J_2]$ . The elements of  $[\mathbf{v}]$  and  $[\mathbf{K}]$  are listed, respectively, as follows:

$$v_{11} = \left( \bar{u}_1 - J_1 F_1 + \frac{1}{h_1} J_1 G_1 \right) \text{Pe}_1, \quad (22)$$

$$v_{12} = J_1 F_1 \text{Pe}_1 - \frac{1}{h_1} J_1 G_2 \text{Pe}_2, \quad (23)$$

$$v_{21} = -\frac{1}{h_2} J_2 G_1 \text{Pe}_1 - J_2 F_2 \text{Pe}_2, \quad (24)$$

$$v_{22} = \left( \bar{u}_2 + J_2 F_2 + \frac{1}{h_2} J_2 G_2 \right) \text{Pe}_2, \quad (25)$$

$$K_{11} = 1 + (-E_1 + J_1 F_1 G_1) \text{Pe}_1^2 = 1 + \kappa_{11} \text{Pe}_1^2, \quad (26)$$

$$K_{12} = (-J_1 F_1 G_2) \text{Pe}_1 \text{Pe}_2 = \kappa_{12} \text{Pe}_1 \text{Pe}_2, \quad (27)$$

$$K_{21} = (J_2 F_2 G_1) \text{Pe}_1 \text{Pe}_2 = \kappa_{21} \text{Pe}_1 \text{Pe}_2, \quad (28)$$

$$K_{22} = 1 + (-E_2 - J_2 F_2 G_2) \text{Pe}_2^2 = 1 + \kappa_{22} \text{Pe}_2^2, \quad (29)$$

where  $v_{11}$  and  $v_{22}$  (which can take positive and negative values) are the two main or principal diagonal elements of  $[\mathbf{v}]$  while  $v_{12}$  and  $v_{21}$  (which can take positive and negative values) are the two off-diagonal elements of  $[\mathbf{v}]$ , and  $K_{11}$  and  $K_{22}$  are the two main or principal diagonal elements of  $[\mathbf{K}]$  while  $K_{12}$  and  $K_{21}$  are the two off-diagonal elements of  $[\mathbf{K}]$ .

It is noted that  $\kappa_{11}$  and  $\kappa_{22}$  in Eqs. (26) and (29) are the coefficients of the first and second main (or principal) diagonal elements of the dispersion tensor, and they always remain positive. In addition,  $\kappa_{12}$  and  $\kappa_{21}$  in Eqs. (27) and (28) are the coefficients of the first and second off-diagonal elements of the dispersion tensor, and they can take positive and negative values.

The developed mathematical model in this study can be reduced to four special cases considering the magnitude of the Darcy numbers in strata 1 and 2 based on the thickness of individual porous layers, as shown in Fig. 2. These special cases are listed and described in Appendix A.

### III. RESULTS

#### A. Description of dispersion tensor

Equations (26)–(29) reveal that the elements of the dispersion tensor ( $K_{11}$ ,  $K_{12}$ ,  $K_{21}$ , and  $K_{22}$ ) are functions of  $\text{Da}_1^*$ ,  $\text{Da}_{1/2}^*$ , the nondimensional thickness ( $h_1 = 1 - h_2$ ), and  $D_{1/2} \phi_{1/2}$ , through the values of  $\kappa_{11}$ ,  $\kappa_{12}$ ,  $\kappa_{21}$ , and  $\kappa_{22}$ , respectively. Hence, the elements of the dispersion tensor are

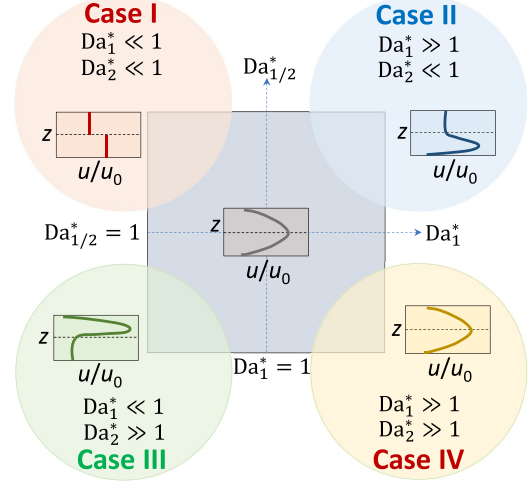


FIG. 2. Special cases I–IV for the developed mathematical model based on the magnitude of  $\text{Da}_1^*$  and  $\text{Da}_2^*$ .

evaluated through the values of  $\kappa_{11}$ ,  $\kappa_{12}$ ,  $\kappa_{21}$ , and  $\kappa_{22}$ . It is noted that the effects of the  $D_{1/2}$  and  $\phi_{1/2}$  on  $\kappa_{ij}$  values are the same since they appear together in the dispersion tensor equations. Therefore, only the role of the  $D_{1/2}$  is discussed.

Figure 3 shows the values of  $\kappa_{11}$ ,  $\kappa_{12}$ ,  $\kappa_{21}$ , and  $\kappa_{22}$  versus  $\text{Da}_1^*$  for several  $h_1$  (including 0.1, 0.3, 0.5, 0.7, and 0.9) and  $\text{Da}_{1/2}^*$  (including 0.01, 0.1, 1, 10, and 100) at  $D_{1/2} = \phi_{1/2} = 1$ . As it is observed, the value of  $\kappa_{11}$  as a function of  $\text{Da}_1^*$  demonstrates a monotonic behavior with respect to  $h_1$  for  $\text{Da}_{1/2}^* \leq 1$ . In other words, the value of  $\kappa_{11}$  against  $\text{Da}_1^*$  will decrease if the nondimensional thickness of layer 1 increases for  $\text{Da}_{1/2}^* \leq 1$ . However, the value of  $\kappa_{11}$  versus  $\text{Da}_1^*$  behaves nonmonotonically with respect to  $h_1$  for  $\text{Da}_{1/2}^* > 1$ .

The results show that the values of  $\kappa_{12}$  and  $\kappa_{21}$  against  $\text{Da}_1^*$  show a nonmonotonic behavior with respect to  $h_1$  for all Darcy number ratios. The results revealed that only for the case of  $h_1 = h_2 = 0.5$  and  $D_{1/2} = \phi_{1/2} = 1$  are the values of  $\kappa_{12}$  and  $\kappa_{21}$  versus  $\text{Da}_1^*$  for all Darcy number ratios symmetric (where  $\kappa_{12} = \kappa_{21}$ ). Otherwise, the  $\kappa_{ij}$  matrix is not symmetric ( $\kappa_{12} \neq \kappa_{21}$ ). At low Darcy number ratios, the off-diagonal elements,  $\kappa_{12}$  and  $\kappa_{21}$ , against  $\text{Da}_1^*$  are negative for small values of  $h_1$  while they are positive for large values of  $h_1$ . As shown in Fig. 3, the value of  $\kappa_{22}$  as a function of  $\text{Da}_1^*$  exhibits monotonic behavior with respect to  $h_1$  for all Darcy number ratios.

To further demonstrate the behavior of the  $\kappa_{ij}$  matrix, Fig. 4 depicts the contour plots for the values of  $\kappa_{ij}$  versus  $\text{Da}_1^*$  and  $\text{Da}_{1/2}^*$  for several  $h_1$  (including 0.1, 0.3, 0.5, 0.7, and 0.9) at  $D_{1/2} = \phi_{1/2} = 1$ , which confirms the results observed from Fig. 3. The results reveal nonmonotonicity of  $\kappa_{ij}$  and the fact that the off-diagonal elements of  $\kappa_{ij}$  could take negative values. These observations are important as they may lead to the manifestation of osmotic dispersion, uphill dispersion, and dispersion barrier, which will be discussed in the next section.

Figure 5 depicts the plots of  $\kappa_{11}$ ,  $\kappa_{12}$ ,  $\kappa_{21}$ , and  $\kappa_{22}$  versus  $\text{Da}_1^*$  for several  $D_{1/2}$  (including 0.01, 0.1, 1, 10, and 100) and  $h_1$  (including 0.1, 0.3, 0.5, 0.7, and 0.9) at  $\text{Da}_{1/2}^* = 0.01$  and  $\phi_{1/2} = 1$ . It is generally observed that  $\kappa_{11}$  as a function of  $\text{Da}_1^*$  becomes larger when the diffusion coefficient ratio increases. This implies a monotonic behavior of  $\kappa_{11}$  against  $\text{Da}_1^*$  with

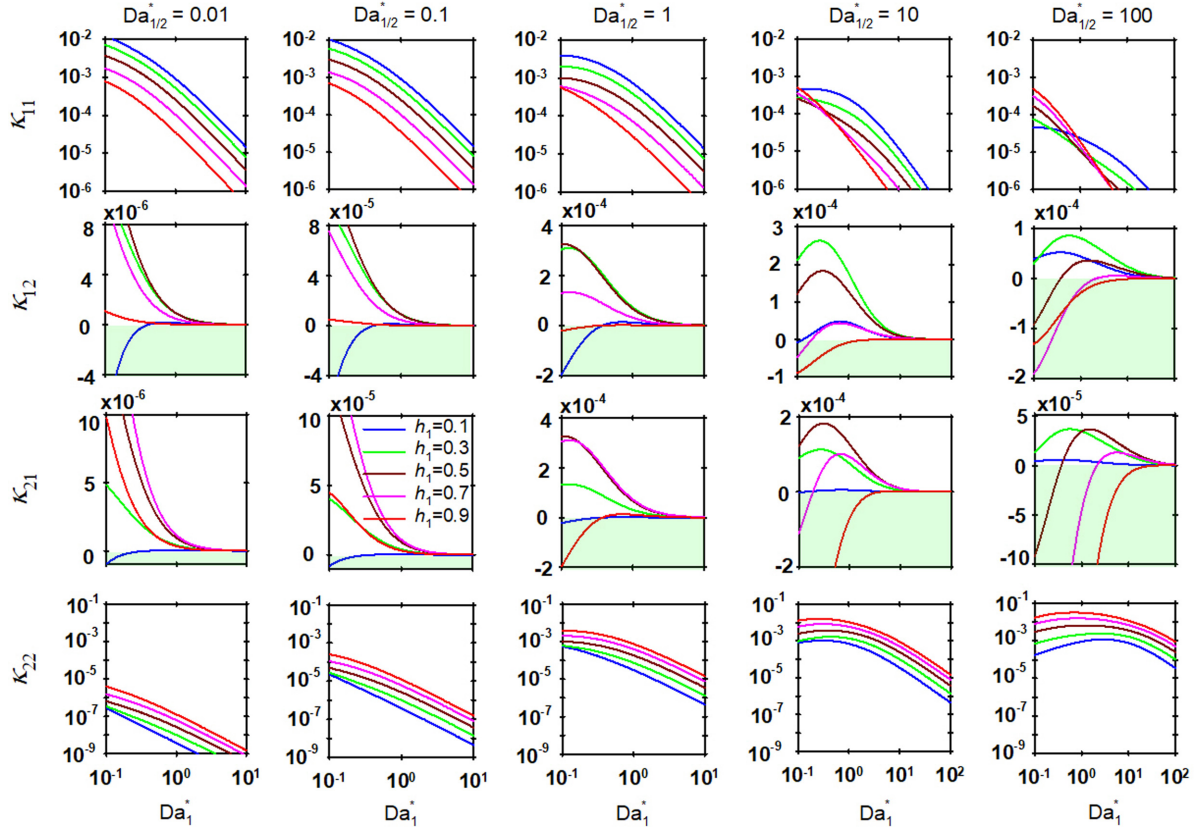


FIG. 3. The values of  $\kappa_{11}$ ,  $\kappa_{12}$ ,  $\kappa_{21}$ , and  $\kappa_{22}$  versus  $Da_1^*$  for several  $h_1$  (including 0.1, 0.3, 0.5, 0.7, and 0.9) and  $Da_{1/2}^*$  (including 0.01, 0.1, 1, 10, and 100) at  $D_{1/2} = \phi_{1/2} = 1$ . The light green shaded area shows the  $Da_1^*$  in which  $\kappa_{12}$  and  $\kappa_{21}$  are negative.

respect to  $D_{1/2}$ . It is worth noting that  $\kappa_{11}$  against  $Da_1^*$  remains almost constant by changing the diffusivity ratio.

It is demonstrated in Fig. 5 that  $\kappa_{12}$  and  $\kappa_{21}$  versus  $Da_1^*$  behave nonmonotonically with respect to the diffusion coefficient ratio for  $h_1 = 0.1$ , where they can take negative values. However,  $\kappa_{12}$  and  $\kappa_{21}$  against  $Da_1^*$  exhibit monotonic behavior with respect to  $D_{1/2}$  for  $h_1 > 0.1$ . The results show that  $\kappa_{12}$  and  $\kappa_{21}$  versus  $Da_1^*$  behave differently for  $h_1 > 0.1$  such that  $\kappa_{12}$  decreases by increasing  $D_{1/2}$  while  $\kappa_{21}$  increases. Again, only for the case of  $h_1 = h_2 = 0.5$  and  $D_{1/2} = \phi_{1/2} = 1$ , the values of  $\kappa_{12}$  and  $\kappa_{21}$  versus  $Da_1^*$  are symmetric (where  $\kappa_{12} = \kappa_{21}$ ). Otherwise, the coefficients of the first and second off-diagonal elements of the dispersion tensor with respect to  $Da_1^*$  are not symmetric (where  $\kappa_{12} \neq \kappa_{21}$ ).

The dispersive fluxes of the injected tracer in layers 1 and 2 can be written as  $\Gamma_1^{\text{dis}} = -\kappa_{11}\text{Pe}_1^2\partial\bar{c}_1/\partial x - \kappa_{12}\text{Pe}_1\text{Pe}_2\partial\bar{c}_2/\partial x$  and  $\Gamma_2^{\text{dis}} = -\kappa_{21}\text{Pe}_1\text{Pe}_2\partial\bar{c}_1/\partial x - \kappa_{22}\text{Pe}_2^2\partial\bar{c}_2/\partial x$ , respectively. Based on Fick's first law, the diffusional mass transfer is normal when the flux of a chemical species and its concentration gradient have opposite signs. However, when the dispersion tensor has a tensorial form, concentration gradient and flux may have similar signs leading to non-normal dispersion. Furthermore, advective fluxes in the first and second layers can be expressed by  $\Gamma_1^{\text{adv}} = v_{11}\bar{c}_1 + v_{12}\bar{c}_2$  and  $\Gamma_2^{\text{adv}} = v_{21}\bar{c}_1 + v_{22}\bar{c}_2$ , respectively. Normally, the advection flux is positive. However,  $v_{11}$ ,  $v_{12}$ ,  $v_{21}$ , and  $v_{22}$  may take negative values resulting in countercurrent advective flux of a chemical species in one of the layers.

The results in Figs. 3–5 revealed that the value of  $\kappa_{12}$  can be nonzero ( $\kappa_{12} \neq 0$ ). This observation indicates when the tracer concentration gradient in layer 1 is absent ( $\partial\bar{c}_1/\partial x = 0$ ), the tracer concentration gradient in layer 2 may lead to a dispersive flux of a tracer in layer 1 ( $\Gamma_1^{\text{dis}} = -\kappa_{12}\text{Pe}_1\text{Pe}_2\partial\bar{c}_2/\partial x \neq 0$  when  $\partial\bar{c}_1/\partial x = 0$ ). This implies the appearance of transport phenomenon called the osmotic dispersion, which is analogous to the osmotic diffusion encountered in the multicomponent molecular diffusion [28–30] and in the binary mixture adsorption in nanoporous media [31]. It will be shown that the osmotic dispersion flux can be positive ( $\Gamma_1^{\text{dis}} > 0$  for positive osmotic dispersion) or negative ( $\Gamma_1^{\text{dis}} < 0$  for negative osmotic dispersion). Similar to  $\kappa_{12}$ , the results in Figs. 3–5 revealed that the value of  $\kappa_{21}$  can be nonzero ( $\kappa_{21} \neq 0$ ), suggesting that if the tracer concentration gradient in the upper layer is absent ( $\partial\bar{c}_2/\partial x = 0$ ), the tracer concentration gradient in the lower layer will cause a dispersive flux of a tracer in the upper layer ( $\Gamma_2^{\text{dis}} = -\kappa_{21}\text{Pe}_1\text{Pe}_2\partial\bar{c}_1/\partial x \neq 0$  when  $\partial\bar{c}_2/\partial x = 0$ ).

As mentioned above and evident from Figs. 3–5,  $\kappa_{12}$  versus  $Da_1^*$  can take negative values, which is more obvious at small values of  $D_{1/2}$ . This may result in a dispersive flux of a tracer in a direction opposite to that which is governed by its own concentration gradient in the lower stratum such that  $\Gamma_1^{\text{dis}} = -\kappa_{11}\text{Pe}_1^2\partial\bar{c}_1/\partial x - \kappa_{12}\text{Pe}_1\text{Pe}_2\partial\bar{c}_2/\partial x > 0$  while  $\partial\bar{c}_1/\partial x > 0$  or  $\Gamma_1^{\text{dis}} = -\kappa_{11}\text{Pe}_1^2\partial\bar{c}_1/\partial x - \kappa_{12}\text{Pe}_1\text{Pe}_2\partial\bar{c}_2/\partial x < 0$  while  $\partial\bar{c}_1/\partial x < 0$ . This suggests a transport phenomenon called the uphill dispersion, analogous to the uphill

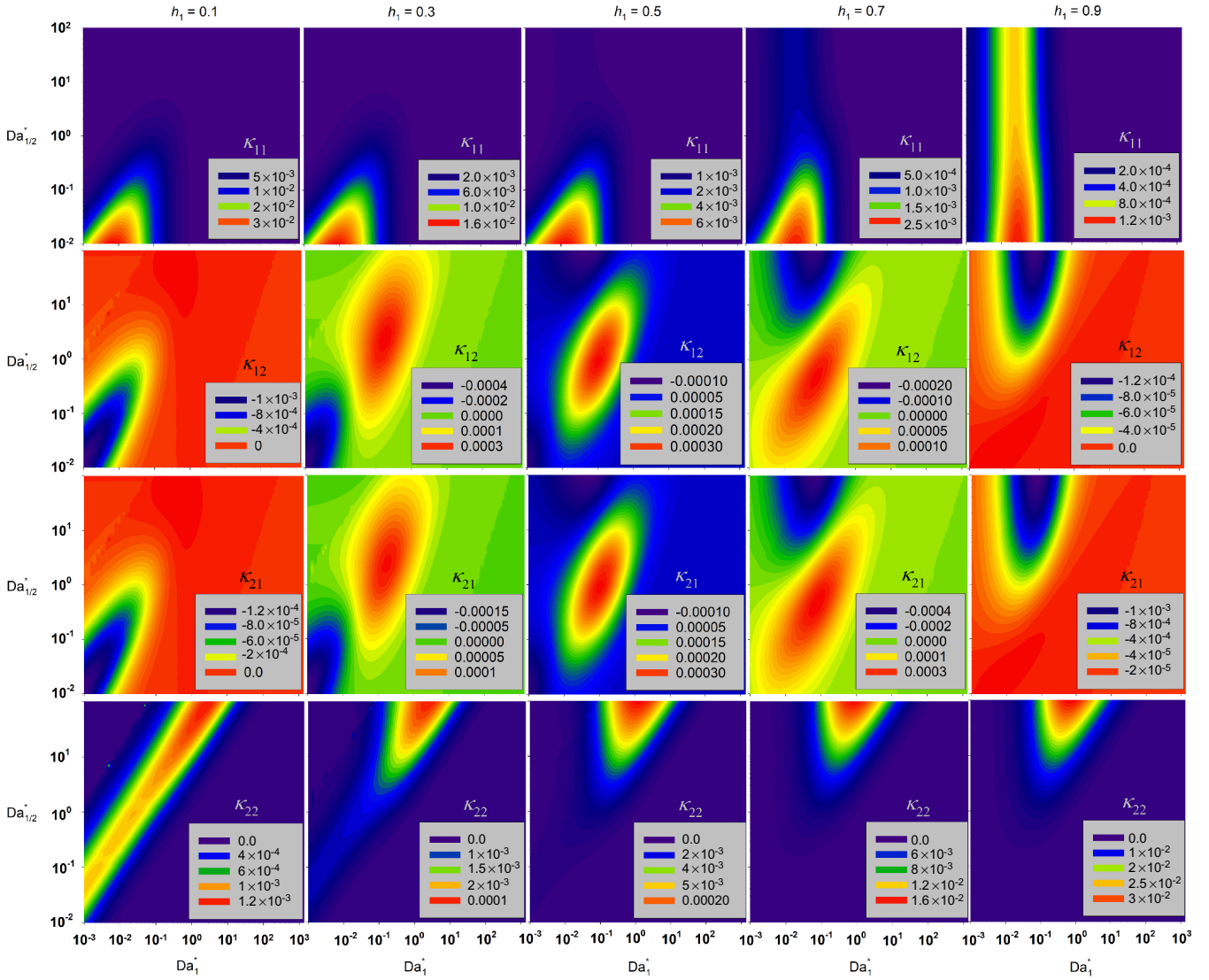


FIG. 4. The contour plots for the values of  $\kappa_{11}$ ,  $\kappa_{12}$ ,  $\kappa_{21}$ , and  $\kappa_{22}$  versus  $Da_1^*$  and  $Da_{1/2}^*$  for several  $h_1$  (including 0.1, 0.3, 0.5, 0.7, and 0.9) at  $D_{1/2} = \phi_{1/2} = 1$ .

diffusion encountered in the multicomponent molecular diffusion [28–30] and in the binary mixture adsorption in nanoporous media [31]. It will be shown that the uphill dispersion flux can be positive ( $\Gamma_1^{\text{dis}} > 0$  for positive uphill dispersion) or negative ( $\Gamma_1^{\text{dis}} < 0$  for negative uphill dispersion).

Similar to  $\kappa_{12}$ , the results in Figs. 3–5 revealed that  $\kappa_{21}$  as a function of  $Da_1^*$  may take a negative value, which is more noticeable at large values of  $D_{1/2}$ . This may cause a dispersive flux of a tracer in a direction opposite to its concentration gradient in layer 2 such that  $\Gamma_2^{\text{dis}} = -\kappa_{21}Pe_1Pe_2\partial\bar{c}_1/\partial x - \kappa_{22}Pe_2^2\partial\bar{c}_2/\partial x > 0$  while  $\partial\bar{c}_2/\partial x > 0$  or  $\Gamma_2^{\text{dis}} = -\kappa_{21}Pe_1Pe_2\partial\bar{c}_1/\partial x - \kappa_{22}Pe_2^2\partial\bar{c}_2/\partial x < 0$  while  $\partial\bar{c}_2/\partial x < 0$ , leading to uphill dispersion.

The results shown in Figs. 3–5 also suggest the possibility of a zero flux of tracer in both layers. A zero dispersion flux of a tracer in layer 1 implies  $\kappa_{11}Pe_1^2\partial\bar{c}_1/\partial x = -\kappa_{12}Pe_1Pe_2\partial\bar{c}_2/\partial x$  ( $\Gamma_1^{\text{dis}} = 0$ ). Similarly, the results suggest the likelihood of zero dispersion flux of the tracer in the

second layer, or  $\kappa_{22}Pe_2^2\partial\bar{c}_2/\partial x = -\kappa_{21}Pe_1Pe_2\partial\bar{c}_1/\partial x$  ( $\Gamma_2^{\text{dis}} = 0$ ). The possibility of zero dispersion flux suggests a dispersion barrier, which is equivalent to a diffusion barrier in multicomponent molecular diffusion [28–30] and in the binary mixture adsorption in nanoporous media [31].

## B. Numerical simulation of tracer transport in stratified porous media

The results discussed in the previous section indicated the possibility of dispersion barrier, uphill dispersion, and osmotic dispersion. To examine the manifestation of these unique transport processes, we conducted numerical simulations of an instantaneous tracer injection into a stratified porous medium based on the developed reduced-order model. A fully implicit finite difference (FD) method is implemented to numerically solve Eqs. (A42) and (A43) subject to the initial and boundary conditions in Eqs. (A44) and (A45). The FD discretization gives a heptadiagonal sparse matrix, and

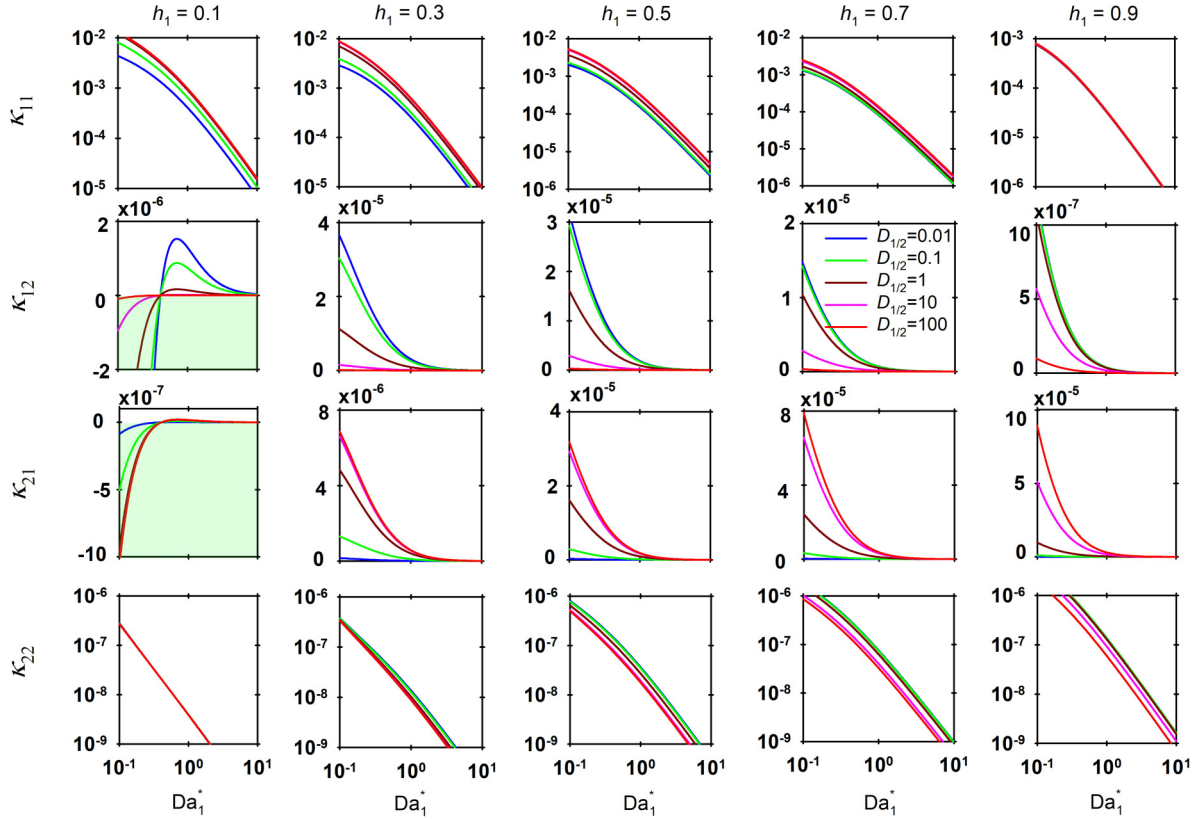


FIG. 5. The plots of  $\kappa_{11}$ ,  $\kappa_{12}$ ,  $\kappa_{21}$ , and  $\kappa_{22}$  versus  $Da_1^*$  for several  $D_{1/2}$  (including 0.01, 0.1, 1, 10, and 100) and  $h_1$  (including 0.1, 0.3, 0.5, 0.7, and 0.9) at  $Da_{1/2}^* = 0.01$  and  $\phi_{1/2} = 1$ . The light green shaded area shows the  $Da_1^*$  in which  $\kappa_{12}$  and  $\kappa_{21}$  are negative.

the GBAND solver is utilized to solve the resultant system of equations [32].

Figures 6(a) and 6(d) show the nondimensional average tracer concentrations in layers 1 and 2 versus the distance from the inlet of stratified porous media at  $t = 12$  for scenario 1, where the coefficients of the two off-diagonal elements of the dispersion tensor are negative while all elements of the matrix of coefficients of the advection term are positive. The dimensionless time necessary for the transverse variation of the tracer concentration to die down to  $1/e$  of its initial value is  $t \approx 1/\pi^2$  [1]. Therefore, a dimensionless time of  $t = 12$  is used to ensure the validity of the major assumption of Taylor dispersion theory for Péclet numbers of  $Pe_1 = 100$  and  $Pe_2 = 1000$  [33,34]. It is noted that the yellow circle denotes the inlet of stratified porous media and the black circle indicates the downstream region of stratified porous media, where the tracer concentration gradient vanishes. In the absence of the interface between the two layers, the tracer concentrations in both layers follow a well-known Gaussian profile. However, the strong coupling between the two layers through the interface and their property contrast leads to interesting transport processes, which are analogous to the ones during the multicomponent molecular diffusion [28–30] and the binary mixture adsorption in nanoporous media [31].

As noted earlier, according to the first Fick's law, the diffusion or dispersion flux of a chemical species is called normal when  $\partial\bar{c}/\partial x$  and flux are opposite in sign. Figure 6(b) shows the trajectory for the dispersive flux,  $\Gamma_1^{\text{dis}}$ , versus

$-\partial\bar{c}_1/\partial x$  in layer 1, where several dispersion regimes are recognized. It is noted that the colored circles in Fig. 6(b) refer to those demonstrated in Fig. 6(a). As the tracer moves along porous medium 1, the dispersive flux trajectory first reveals the normal dispersion, where  $\Gamma_1^{\text{dis}} < 0$  and  $-\partial\bar{c}_1/\partial x < 0$  (blue curve). This continues until the dispersive flux becomes zero, which identifies the dispersion barrier,  $\kappa_{11}Pe_1^2\partial\bar{c}_1/\partial x = -\kappa_{12}Pe_1Pe_2\partial\bar{c}_2/\partial x$  ( $\Gamma_1^{\text{dis}} = 0$ ) while  $-\partial\bar{c}_1/\partial x < 0$ , as shown by the red circle in Fig. 6(b). Thereafter, the dispersive flux trajectory for the tracer in layer 1 is positive,  $\Gamma_1^{\text{dis}} > 0$ , while  $-\partial\bar{c}_1/\partial x < 0$ , suggesting that the dispersive flux and the concentration gradient of the tracer in layer 1 are against each other. This regime is called the positive uphill dispersion since  $\Gamma_1^{\text{dis}} > 0$ , as illustrated by the pink curve in Fig. 6(b), and continues until the dispersive flux of the tracer reaches  $\partial\bar{c}_1/\partial x = 0$ . This gives a nonzero positive dispersive flux ( $\Gamma_1^{\text{dis}} = -\kappa_{12}Pe_1Pe_2\partial\bar{c}_2/\partial x \neq 0$ ) when the concentration gradient of the tracer in layer 1 is absent ( $\partial\bar{c}_1/\partial x = 0$ ). This regime is called the positive osmotic dispersion since  $\Gamma_1^{\text{dis}} > 0$ , as shown by the green circle in Fig. 6(b). Subsequently, the dispersive flux trajectory reveals the normal dispersion, where  $\Gamma_1^{\text{dis}} > 0$  and  $-\partial\bar{c}_1/\partial x > 0$  (blue curve). This continues until the dispersive flux becomes zero, which identifies the dispersion barrier,  $\kappa_{11}Pe_1^2\partial\bar{c}_1/\partial x = -\kappa_{12}Pe_1Pe_2\partial\bar{c}_2/\partial x$  ( $\Gamma_1^{\text{dis}} = 0$ ) while  $-\partial\bar{c}_1/\partial x > 0$ , as shown by the red circle in Fig. 6(b). Finally, the dispersive flux trajectory for the tracer in layer 1 is negative,  $\Gamma_1^{\text{dis}} < 0$ , while  $-\partial\bar{c}_1/\partial x < 0$ , suggesting that the dispersive flux and the concentration gradient of the tracer

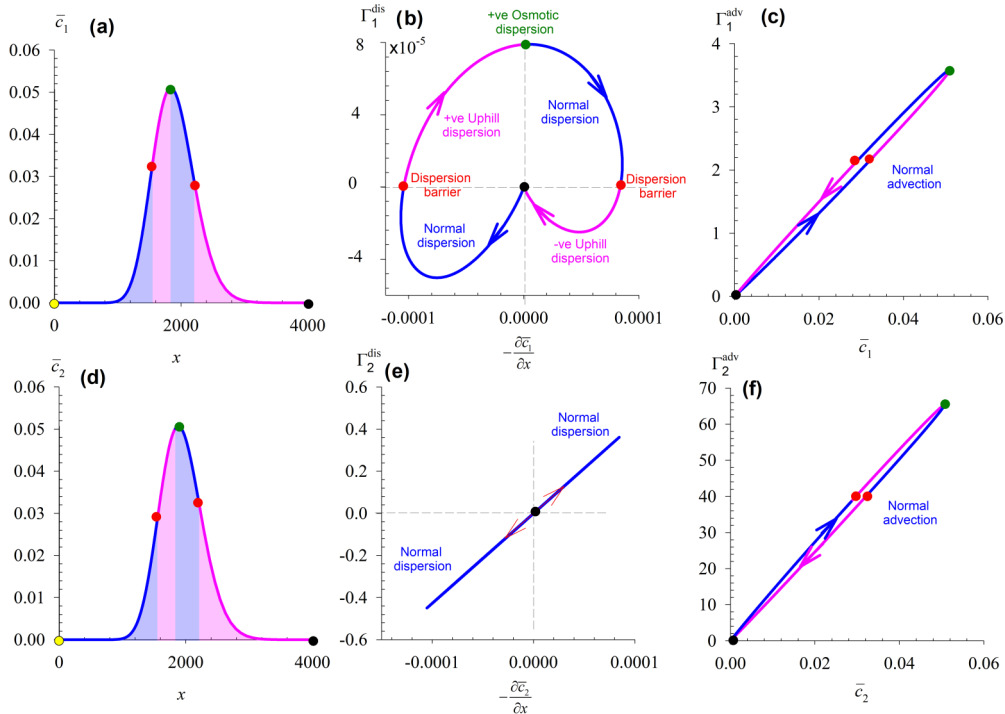


FIG. 6. Results for scenario 1 with  $Pe_1 = 100$ ,  $Pe_2 = 1000$ ,  $h_1 = 0.75$ ,  $Da_1^* = 0.1$ ,  $Da_2^* = 10$ ,  $D_{1/2} = 0.1$ ,  $\phi_{1/2} = 50$ ,  $v_{ij} = \begin{bmatrix} 45.33 & 25.30 \\ 380.12 & 909.27 \end{bmatrix}$ , and  $\kappa_{ij} = \begin{bmatrix} 3.92 \times 10^{-4} & -3.89 \times 10^{-5} \\ -5.83 \times 10^{-4} & 4.33 \times 10^{-3} \end{bmatrix}$  (where  $i, j = 1, 2$ ). (a), (d) The nondimensional average tracer concentrations in layers 1 and 2,  $\bar{c}_1$  and  $\bar{c}_2$ , versus the distance from the inlet of stratified porous media,  $x$ , at  $t = 12$ . (b), (e) The dispersive fluxes,  $\Gamma_1^{\text{dis}}$  and  $\Gamma_2^{\text{dis}}$ , versus  $-\partial\bar{c}_1/\partial x$  and  $-\partial\bar{c}_2/\partial x$  in layers 1 and 2, respectively. (c), (f) The advective fluxes,  $\Gamma_1^{\text{adv}}$  and  $\Gamma_2^{\text{adv}}$ , versus the nondimensional average tracer concentrations,  $\bar{c}_1$  and  $\bar{c}_2$ , in layers 1 and 2, respectively. Colored circles in (b), (c) refer to those in (a) and colored circles in (e), (f) refer to those in (d). The blue and pink curves in (b), (e) denote the normal dispersion and the uphill dispersion, respectively, and the arrows show the direction of tracer transport.

in layer 1 are against each other. This regime is called the negative uphill dispersion since  $\Gamma_1^{\text{dis}} < 0$ , as illustrated by the pink curve in Fig. 6(b). The dispersive flux for the tracer in layer 2, which is shown in Fig. 6(e), remains normal ( $\Gamma_2^{\text{dis}} > 0$  when  $-\partial\bar{c}_2/\partial x > 0$  or  $\Gamma_2^{\text{dis}} < 0$  when  $-\partial\bar{c}_2/\partial x < 0$ ).

Figures 6(c) and 6(f) illustrate the trajectories for the advective fluxes,  $\Gamma_1^{\text{adv}}$  and  $\Gamma_2^{\text{adv}}$ , versus the nondimensional average tracer concentrations,  $\bar{c}_1$  and  $\bar{c}_2$ , in layers 1 and 2, respectively. The results reveal that the advective fluxes in both strata remain normal ( $\Gamma_1^{\text{adv}} = v_{11}\bar{c}_1 + v_{12}\bar{c}_2 > 0$  and  $\Gamma_2^{\text{adv}} = v_{21}\bar{c}_1 + v_{22}\bar{c}_2 > 0$ ), but the advective flux in layer 2 is larger than the advective flux in stratum 1 ( $\Gamma_2^{\text{adv}} > \Gamma_1^{\text{adv}}$ ).

Figure 7 presents the results of scenario 2, where the coefficients of the two off-diagonal elements of the dispersion tensor are negative while all elements of the matrix of coefficients of the advection term are positive. Similar to the former scenario, the tracer concentrations in both layers follow a well-known Gaussian profile, as shown by  $\bar{c}_1$  and  $\bar{c}_2$  profiles in Figs. 7(a) and 7(d). For this scenario, as depicted in Fig. 7(b), the dispersion regimes in layer 1 evolve in the order of the positive uphill dispersion ( $\Gamma_1^{\text{dis}} > 0$  when  $-\partial\bar{c}_1/\partial x < 0$ ), the positive osmotic dispersion ( $\Gamma_1^{\text{dis}} \neq 0$  when  $\partial\bar{c}_1/\partial x = 0$ ), the normal dispersion ( $\Gamma_1^{\text{dis}} > 0$  when  $-\partial\bar{c}_1/\partial x > 0$ ), the dispersion barrier ( $\Gamma_1^{\text{dis}} = 0$  when  $-\partial\bar{c}_1/\partial x > 0$ ), and the negative uphill dispersion ( $\Gamma_1^{\text{dis}} < 0$  when  $-\partial\bar{c}_1/\partial x > 0$ ). The sequence of the dispersion regimes along layer 1 in the former scenario, Fig. 6(b),

was the normal dispersion ( $\Gamma_1^{\text{dis}} < 0$  when  $-\partial\bar{c}_1/\partial x < 0$ ), the dispersion barrier ( $\Gamma_1^{\text{dis}} = 0$  when  $-\partial\bar{c}_1/\partial x < 0$ ), the positive uphill dispersion ( $\Gamma_1^{\text{dis}} > 0$  when  $-\partial\bar{c}_1/\partial x < 0$ ), the positive osmotic dispersion ( $\Gamma_1^{\text{dis}} \neq 0$  when  $\partial\bar{c}_1/\partial x = 0$ ), the normal dispersion ( $\Gamma_1^{\text{dis}} > 0$  when  $-\partial\bar{c}_1/\partial x > 0$ ), the dispersion barrier ( $\Gamma_1^{\text{dis}} = 0$  when  $-\partial\bar{c}_1/\partial x > 0$ ), and the negative uphill dispersion ( $\Gamma_1^{\text{dis}} < 0$  when  $-\partial\bar{c}_1/\partial x > 0$ ). The dispersive flux for the tracer in layer 2, which is shown in Fig. 7(e), remains normal ( $\Gamma_2^{\text{dis}} > 0$  when  $-\partial\bar{c}_2/\partial x > 0$  or  $\Gamma_2^{\text{dis}} < 0$  when  $-\partial\bar{c}_2/\partial x < 0$ ). It is revealed from Figs. 7(c) and 7(f) that the advective fluxes in both layers remain normal ( $\Gamma_1^{\text{adv}} > 0$  and  $\Gamma_2^{\text{adv}} > 0$ ), but the advective flux in layer 2 is larger than the advective flux in layer 1 ( $\Gamma_2^{\text{adv}} > \Gamma_1^{\text{adv}}$ ).

In the last simulated scenario (scenario 3), the coefficients of the two off-diagonal elements of the dispersion tensor and the two off-diagonal elements of the matrix of coefficients of the advection term are negative. Similar to scenarios 1 and 2, the tracer concentrations in both layers follow a well-known Gaussian profile, as shown by the  $\bar{c}_1$  and  $\bar{c}_2$  profiles in Figs. 8(a) and 8(d). The results presented in Fig. 8(b) demonstrate that the dispersive flux for the tracer in layer 1 remains normal ( $\Gamma_1^{\text{dis}} > 0$  when  $-\partial\bar{c}_1/\partial x > 0$  or  $\Gamma_1^{\text{dis}} < 0$  when  $-\partial\bar{c}_1/\partial x < 0$ ). It is observed from Fig. 8(e) that the dispersive flux for the tracer in layer 2 indicates the negative ( $\Gamma_2^{\text{dis}} < 0$  when  $-\partial\bar{c}_2/\partial x > 0$ ) and positive ( $\Gamma_2^{\text{dis}} > 0$  when  $-\partial\bar{c}_2/\partial x < 0$ ) uphill dispersions for the whole trajectory. Figure 8(c) illustrates that the

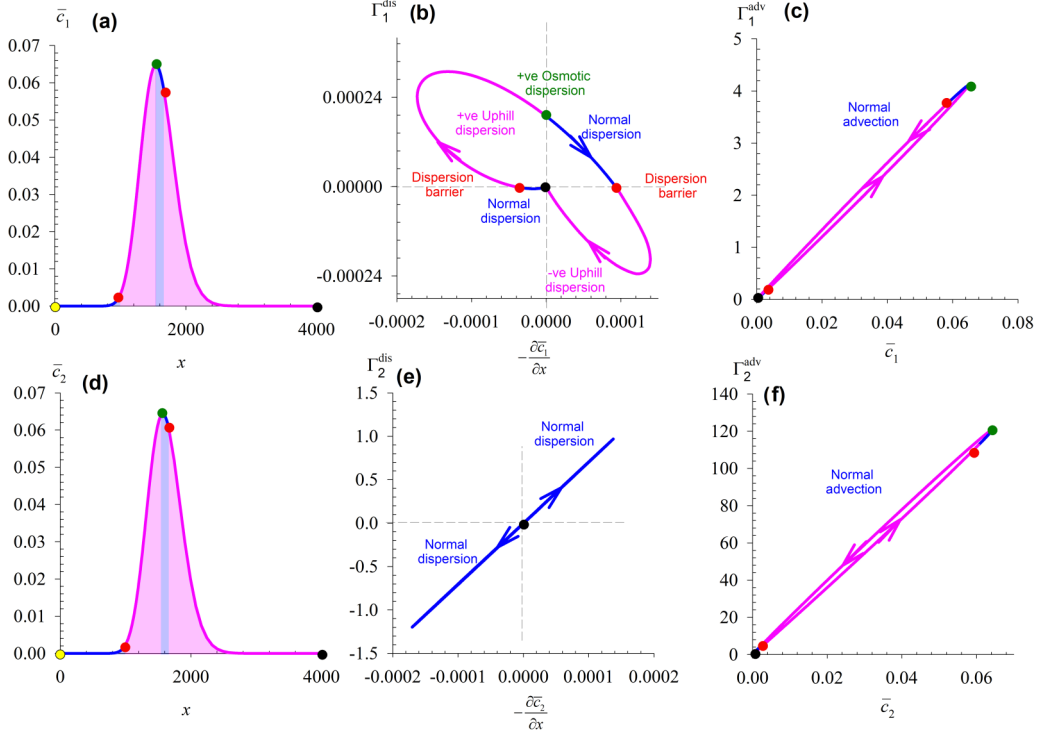


FIG. 7. Results for scenario 2 with  $Pe_1 = 100$ ,  $Pe_2 = 1000$ ,  $h_1 = 0.85$ ,  $Da_1^* = 0.1$ ,  $Da_2^* = 10$ ,  $D_{1/2} = 0.1$ ,  $\phi_{1/2} = 50$ ,  $v_{ij} = \begin{bmatrix} 44.82 & 18.80 \\ 533.40 & 1346.15 \end{bmatrix}$ , and  $\kappa_{ij} = \begin{bmatrix} 4.79 \times 10^{-4} & -6.37 \times 10^{-5} \\ -1.80 \times 10^{-3} & 7.21 \times 10^{-3} \end{bmatrix}$  (where  $i, j = 1, 2$ ). (a), (d) The nondimensional average tracer concentrations in layers 1 and 2,  $\bar{c}_1$  and  $\bar{c}_2$ , versus the distance from the inlet of stratified porous media,  $x$ , at  $t = 12$ . (b), (e) The dispersive fluxes,  $\Gamma_1^{\text{dis}}$  and  $\Gamma_2^{\text{dis}}$ , versus  $-\partial\bar{c}_1/\partial x$  and  $-\partial\bar{c}_2/\partial x$  in layers 1 and 2, respectively. (c), (f) The advective fluxes,  $\Gamma_1^{\text{adv}}$  and  $\Gamma_2^{\text{adv}}$ , versus the nondimensional average tracer concentrations,  $\bar{c}_1$  and  $\bar{c}_2$ , in layers 1 and 2, respectively. Colored circles in (b), (c) refer to those in (a) and colored circles in (e), (f) refer to those in (d). The blue and pink curves in (b), (e) denote the normal dispersion and the uphill dispersion, respectively, and the arrows show the direction of tracer transport.

advective flux in layer 1 remains normal ( $\Gamma_1^{\text{adv}} > 0$ ). In contrast, the advective flux in layer 2, as shown in Fig. 8(f), exhibits the uphill advection ( $\Gamma_2^{\text{adv}} = v_{21}\bar{c}_1 + v_{22}\bar{c}_2 < 0$ ), indicating that the tracer is advecting upstream of the flow or countercurrent.

#### IV. DISCUSSION

The cross-advective and cross-dispersive terms [see Eq. (21)] originate from the continuity of velocity and the corresponding advective flux and the interface. The continuity of velocity and advective flux at the interface, in turn, results in a macroscale velocity profile in the composite two-layer system, where the velocities in layer 1 and layer 2 are not equal at a particular  $x$ . In other words, the macroscale velocity profile becomes a function of longitudinal ( $x$ ) and transverse ( $z$ ) directions. The nonsymmetrical macroscale velocity combined with the nonzero diffusion flux at the interface between the two porous layers leads to cross-advective and cross-dispersion transport in both layers.

The cross-diffusion terms,  $J_1$  and  $J_2$ , [see Eq. (21)] originate from the concentration and diffusion flux continuity at the interface between the two layers. For instance, for the special case I, where individual layer velocity profiles are independent of the transverse direction ( $u_1 = 1$  and  $u_2 = 1$ ), the macroscale velocity profile is only a function of the

longitudinal ( $x$ ) direction. Hence, the cross-advective and cross-dispersion terms are absent, and only the cross-diffusion terms  $J_1$  and  $J_2$  are present.

From a physical point of view, porous media heterogeneities in the form of layering lead to fully developed macroscale velocity profiles that are, in fact, nonsymmetrical. Consequently, tracer transport coupled with a macroscale velocity field can manifest dispersion barrier, uphill dispersion and advection, and osmotic dispersion during tracer transport in stratified porous media, as demonstrated in this work.

For normal dispersion, flux and concentration gradient are opposite in sign implying that if  $\Gamma_1^{\text{dis}} > 0$  then  $\partial\bar{c}_1/\partial x < 0$ . However, for instance, when  $\Gamma_1^{\text{dis}} > 0$  while  $\partial\bar{c}_1/\partial x > 0$  the dispersive transport is not normal. This work shows that a nonsymmetrical macroscale velocity distribution leads to a tensorial dispersion resulting in uphill dispersion.

A concentration gradient is normally required for dispersive transport to occur. Dispersive transport of a chemical species in the absence of concentration or the so-called osmotic dispersion is observed when transport takes place in a fully developed nonsymmetrical macroscale velocity field due to heterogeneities in the form of layering a porous medium. Also, it is shown that a zero-dispersion flux of a tracer (dispersion barrier) may be expected, which again has roots in the coupling of nonsymmetrical macroscale velocity field and tracer transport.

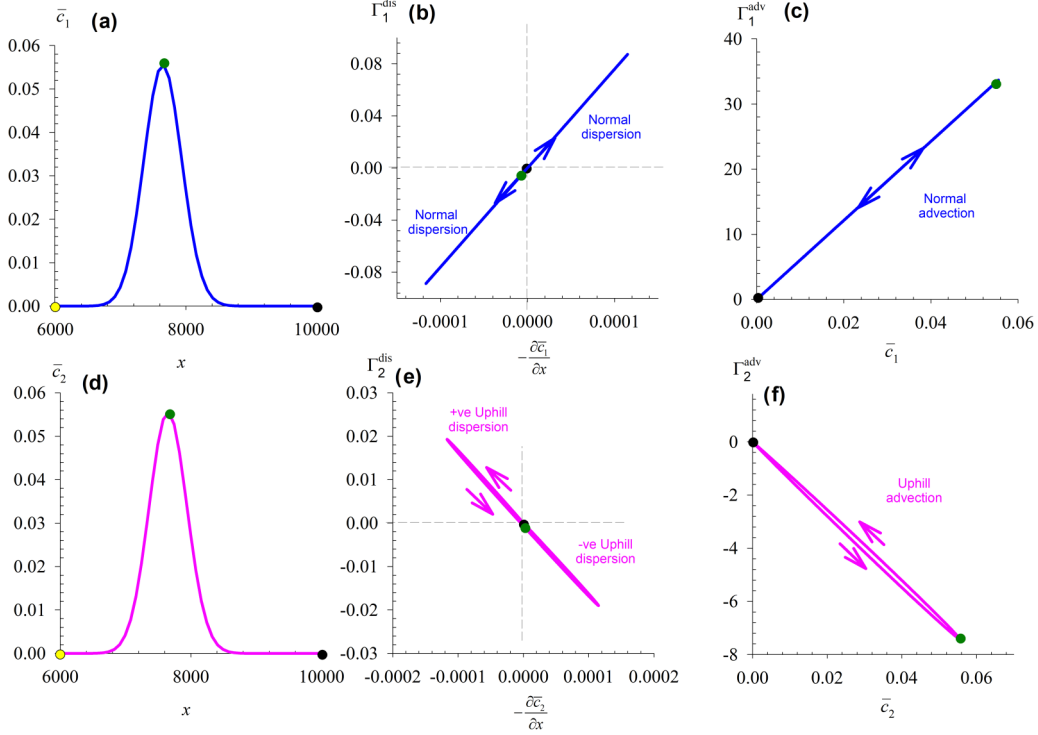


FIG. 8. Results for scenario 3 with  $Pe_1 = 1000$ ,  $Pe_2 = 100$ ,  $h_1 = 0.85$ ,  $Da_1^* = 0.045$ ,  $Da_{12}^* = 10$ ,  $D_{1/2} = 0.1$ ,  $\phi_{1/2} = 50$ ,  $v_{ij} = \begin{bmatrix} 615.49 & -8.84 \\ -250.39 & 116.82 \end{bmatrix}$ , and  $\kappa_{ij} = \begin{bmatrix} 7.67 \times 10^{-4} & -7.31 \times 10^{-5} \\ -2.07 \times 10^{-3} & 4.22 \times 10^{-3} \end{bmatrix}$  (where  $i, j = 1, 2$ ). (a), (d) The nondimensional average tracer concentrations in layers 1 and 2,  $\bar{c}_1$  and  $\bar{c}_2$ , versus the distance from the inlet of stratified porous media,  $x$ , at  $t = 12$ . (b), (e) The dispersive fluxes,  $\Gamma_1^{\text{dis}}$  and  $\Gamma_2^{\text{dis}}$ , versus  $-\partial\bar{c}_1/\partial x$  and  $-\partial\bar{c}_2/\partial x$  in layers 1 and 2, respectively. (c), (f) The advective fluxes,  $\Gamma_1^{\text{adv}}$  and  $\Gamma_2^{\text{adv}}$ , versus the nondimensional average tracer concentrations,  $\bar{c}_1$  and  $\bar{c}_2$ , in layers 1 and 2, respectively. Colored circles in (b), (c) refer to those in (a) and colored circles in (e), (f) refer to those in (d). The blue and pink curves in (b), (e) denote the normal dispersion and the uphill dispersion, respectively, and the arrows show the direction of tracer transport.

The dispersion discussed in our work originates from the velocity gradient (shear dispersion) as is in the Taylor dispersion theory [1]. It is well established that the dispersion originated from shear scales is proportional to  $Pe^2$  [1]. However, the hydrodynamic dispersion in porous media discussed by Gelhar and Axness [35] is the macroscopic consequence of several physical and chemical processes [36], including motion of a chemical species in tortuous flow paths in pore space, velocity gradient in the pore level, porous media heterogeneity, molecular diffusion, variation in thermophysical properties of the fluid, and solid-fluid interaction such as adsorption and desorption [36].

## V. SUMMARY AND CONCLUSIONS

We studied dispersion in stratified porous media using the generalization of the Taylor dispersion theory. First, the fully developed Stokes flow of a Newtonian and incompressible fluid is described by coupling the Darcy-Brinkman equations in the lower and upper porous media subject to the continuity of velocity and shear stress at the interface between two porous layers to obtain the velocity distributions. Next, the advection-diffusion equations in the lower and upper strata are coupled using the continuity of tracer concentration and mass flux at the interface between two strata to address the tracer transport. Then, the reduced-order models

for advection-dispersion tracer transport are derived using the Reynolds decomposition and averaging techniques, which give the matrix of coefficients of the advection term and the dispersion tensor. The evaluation of the resultant dispersion tensor, tracer concentrations, and dispersive and advective fluxes reveal that several transport phenomena of uphill advection and dispersion, dispersion barrier, and osmotic dispersion may be developed due to the presence of an interface between the two porous media with different physical properties. We found that the dispersion has a tensorial characteristic even for a simple two-layer homogenous porous medium. The tensorial nature of dispersion in a stratified porous medium was found to originate from the coupling through the interface and the Stokes flow in the two porous layers. Application of the Taylor dispersion theory to a limiting case of Darcy flow in a stratified porous medium suggests that only a cross-diffusive flux between the two layers leads to mixing and proves the absence of Taylor dispersion. The results suggest that the mixing observed in field scale may not necessarily originate from Taylor dispersion and could be due to the modified advection terms and cross-diffusive flux between the two layers. It was demonstrated that the Taylor dispersion theory can be generalized to obtain dispersion in stratified porous media. The proposed model along with the findings of this study can pave the way for the development of the dispersion tensor in multilayered porous media.

## ACKNOWLEDGMENTS

M.D. is gratefully appreciative of the support from the Department of Petroleum Engineering in the College of Engineering and Applied Science at the University of Wyoming. H.H. acknowledges the support from the Department of Chemical and Petroleum Engineering in the Schulich School of Engineering at the University of Calgary.

## APPENDIX A: MODEL REDUCTION AND SPECIAL CASES

## 1. Reynolds decomposition and averaging methods

The Reynolds decomposition, which is a technique to split the average and fluctuation components of a variable [33], can be used to write the nondimensional velocities and tracer concentrations in porous layers 1 and 2, respectively, as follows:

$$u_1(z) = \bar{u}_1 + u'_1(z) = \frac{1}{h_1} \int_{-h_1}^0 u_1 dz + u'_1(z), \quad (\text{A1})$$

$$u_2(z) = \bar{u}_2 + u'_2(z) = \frac{1}{h_2} \int_0^{h_2} u_2 dz + u'_2(z), \quad (\text{A2})$$

$$\begin{aligned} c_1(x, z, t) &= \bar{c}_1(x, t) + c'_1(x, z, t) \\ &= \frac{1}{h_1} \int_{-h_1}^0 c_1 dz + c'_1(x, z, t), \end{aligned} \quad (\text{A3})$$

$$\begin{aligned} c_2(x, z, t) &= \bar{c}_2(x, t) + c'_2(x, z, t) \\ &= \frac{1}{h_2} \int_0^{h_2} c_2 dz + c'_2(x, z, t), \end{aligned} \quad (\text{A4})$$

where  $\bar{u}_1$ ,  $\bar{u}_2$ ,  $\bar{c}_1$ , and  $\bar{c}_2$  are the nondimensional average velocities and tracer concentrations in porous media 1 and 2, respectively, and  $u'_1$ ,  $u'_2$ ,  $c'_1$ , and  $c'_2$  are the fluctuation components. The averages of the fluctuation components are zero, based on the Reynolds decomposition [33]:

$$\begin{aligned} \frac{1}{h_1} \int_{-h_1}^0 u'_1 dz &= \frac{1}{h_2} \int_0^{h_2} u'_2 dz = \frac{1}{h_1} \int_{-h_1}^0 c'_1 dz \\ &= \frac{1}{h_2} \int_0^{h_2} c'_2 dz = 0. \end{aligned} \quad (\text{A5})$$

The following expressions can be derived for the nondimensional average velocities in strata 1 and 2 using Eqs. (7), (8), (A1), and (A2):

$$\bar{u}_1 = \frac{A_1}{\eta_1 h_1} \sinh(\eta_1 h_1) + \frac{B_1}{\eta_1 h_1} [1 - \cosh(\eta_1 h_1)] + 1, \quad (\text{A6})$$

$$\bar{u}_2 = \frac{A_2}{\eta_2 h_2} \sinh(\eta_2 h_2) + \frac{B_2}{\eta_2 h_2} [\cosh(\eta_2 h_2) - 1] + 1. \quad (\text{A7})$$

## 2. Derivation of reduced-order models for advection-dispersion tracer transport

If  $c_1$  and  $c_2$  from Eqs. (A3) and (A4) are substituted into Eqs. (13)–(20), the following equations can be derived:

$$\begin{aligned} \frac{\partial \bar{c}_1}{\partial t} + \frac{\partial c'_1}{\partial t} + \text{Pe}_1 u_1 \frac{\partial \bar{c}_1}{\partial x} + \text{Pe}_1 u_1 \frac{\partial c'_1}{\partial x} \\ = \frac{\partial^2 \bar{c}_1}{\partial x^2} + \frac{\partial^2 c'_1}{\partial x^2} + \frac{\partial^2 c'_1}{\partial z^2}, \end{aligned} \quad (\text{A8})$$

$$\begin{aligned} D_{1/2} \frac{\partial \bar{c}_2}{\partial t} + D_{1/2} \frac{\partial c'_2}{\partial t} + \text{Pe}_2 u_2 \frac{\partial \bar{c}_2}{\partial x} + \text{Pe}_2 u_2 \frac{\partial c'_2}{\partial x} \\ = \frac{\partial^2 \bar{c}_2}{\partial x^2} + \frac{\partial^2 c'_2}{\partial x^2} + \frac{\partial^2 c'_2}{\partial z^2}, \end{aligned} \quad (\text{A9})$$

$$\begin{aligned} \bar{c}_1(x, t = 0) + c'_1(x, z, t = 0) \\ = \bar{c}_2(x, t = 0) + c'_2(x, z, t = 0) = \delta(x), \end{aligned} \quad (\text{A10})$$

$$\begin{aligned} \bar{c}_1(x \rightarrow \infty, t) + c'_1(x \rightarrow \infty, z, t) \\ = \bar{c}_2(x \rightarrow \infty, t) + c'_2(x \rightarrow \infty, z, t) = 0, \end{aligned} \quad (\text{A11})$$

$$\frac{\partial c'_1(x, z = -h_1, t)}{\partial z} = 0, \quad (\text{A12})$$

$$\bar{c}_1(x, t) + c'_1(x, z = 0, t) = \bar{c}_2(x, t) + c'_2(x, z = 0, t), \quad (\text{A13})$$

$$D_{1/2} \phi_{1/2} \frac{\partial c'_1(x, z = 0, t)}{\partial z} = \frac{\partial c'_2(x, z = 0, t)}{\partial z}, \quad (\text{A14})$$

$$\frac{\partial c'_2(x, z = h_2, t)}{\partial z} = 0. \quad (\text{A15})$$

Averaging Eqs. (A8) and (A9) with the aid of Eqs. (A5), (A12), and (A15) results in

$$\frac{\partial \bar{c}_1}{\partial t} + \text{Pe}_1 \bar{u}_1 \frac{\partial \bar{c}_1}{\partial x} + \text{Pe}_1 u_1 \frac{\partial c'_1}{\partial x} = \frac{\partial^2 \bar{c}_1}{\partial x^2} + \frac{1}{h_1} \frac{\partial c'_1(x, z = 0, t)}{\partial z}, \quad (\text{A16})$$

$$\begin{aligned} D_{1/2} \frac{\partial \bar{c}_2}{\partial t} + \text{Pe}_2 \bar{u}_2 \frac{\partial \bar{c}_2}{\partial x} + \text{Pe}_2 u_2 \frac{\partial c'_2}{\partial x} \\ = \frac{\partial^2 \bar{c}_2}{\partial x^2} - \frac{1}{h_2} \frac{\partial c'_2(x, z = 0, t)}{\partial z}. \end{aligned} \quad (\text{A17})$$

Subtraction of Eqs. (A16) and (A17) from Eqs. (A8) and (A9), respectively, leads to

$$\begin{aligned} \frac{\partial c'_1}{\partial t} + \text{Pe}_1 (u_1 - \bar{u}_1) \frac{\partial \bar{c}_1}{\partial x} + \text{Pe}_1 u_1 \frac{\partial c'_1}{\partial x} - \text{Pe}_1 u_1 \frac{\partial c'_1}{\partial x} \\ = \frac{\partial^2 c'_1}{\partial x^2} + \frac{\partial^2 c'_1}{\partial z^2} - \frac{1}{h_1} \frac{\partial c'_1(x, z = 0, t)}{\partial z}, \end{aligned} \quad (\text{A18})$$

$$\begin{aligned} D_{1/2} \frac{\partial c'_2}{\partial t} + \text{Pe}_2 (u_2 - \bar{u}_2) \frac{\partial \bar{c}_2}{\partial x} + \text{Pe}_2 u_2 \frac{\partial c'_2}{\partial x} - \text{Pe}_2 u_2 \frac{\partial c'_2}{\partial x} \\ = \frac{\partial^2 c'_2}{\partial x^2} + \frac{\partial^2 c'_2}{\partial z^2} + \frac{1}{h_2} \frac{\partial c'_2(x, z = 0, t)}{\partial z}. \end{aligned} \quad (\text{A19})$$

The exact Eqs. (A18) and (A19) are now subjected to the three following assumptions adopted by Taylor [1] and Fischer *et al.* [4] on the tracer transport.

(i)  $\partial c'_1 / \partial t \approx 0$  and  $D_{1/2} \partial c'_2 / \partial t \approx 0$  indicate a quasisteady state condition, which can be considered after passing sufficient time from the tracer introduction at the inlet of the stratified porous media if the fluctuation components in the transversal direction in strata 1 and 2 are smoothed out by the transversal diffusion. This infers that  $\bar{c}_1 \gg c'_1$  and  $\bar{c}_2 \gg c'_2$ , where the average tracer concentrations in layers 1 and 2 become much larger than the fluctuation components. Therefore, the fluctuation components in the transversal direction in porous layers 1 and 2 are negligible. For timescales in the

order of magnitudes of the diffusion times across strata 1 and 2, which are  $H_1^2/D_1$  and  $H_2^2/D_2$ , respectively, this assumption can be taken into consideration.

(ii)  $c'_1$  and  $c'_2$ , which are the fluctuation components in layers 1 and 2, vary slowly. This infers that  $\text{Pe}_1 u_1 \partial c'_1 / \partial x \approx \text{Pe}_1 u_1 \partial c'_1 / \partial x$  and  $\text{Pe}_2 u_2 \partial c'_2 / \partial x \approx \text{Pe}_2 u_2 \partial c'_2 / \partial x$ .

(iii)  $\text{Pe}_1(u_1 - \bar{u}_1) \partial \bar{c}_1 / \partial x \gg \partial^2 c'_1 / \partial x^2$  and  $\text{Pe}_2(u_2 - \bar{u}_2) \partial \bar{c}_2 / \partial x \gg \partial^2 c'_2 / \partial x^2$  show that the longitudinal diffusion can be ignored compared to the longitudinal advection in porous layers 1 and 2. Therefore, the impact of the longitudinal diffusion is not considerable, and the tracer transport in strata 1 and 2 is mainly controlled by the longitudinal advection and the transversal diffusion.

If assumptions (i)–(iii) are used, Eqs. (A18) and (A19) will reduce to

$$\text{Pe}_1(u_1 - \bar{u}_1) \frac{\partial \bar{c}_1}{\partial x} + \frac{1}{h_1} \frac{\partial c'_1(x, z = 0, t)}{\partial z} = \frac{\partial^2 c'_1}{\partial z^2}, \quad (\text{A20})$$

$$\text{Pe}_2(u_2 - \bar{u}_2) \frac{\partial \bar{c}_2}{\partial x} - \frac{1}{h_2} \frac{\partial c'_2(x, z = 0, t)}{\partial z} = \frac{\partial^2 c'_2}{\partial z^2}. \quad (\text{A21})$$

If Eqs. (A20) and (A21) are integrated twice with respect to  $z$  and the resulting expressions are subjected to Eqs. (A5), (A12), and (A15) to find the constants of integrations,  $c'_1$  and  $c'_2$  will be derived as follows:

$$c'_1 = \left[ \left( \frac{z^2}{2} - \frac{h_1^2}{6} + \frac{1}{\eta_1^2} \right) (1 - \bar{u}_1) - \left( \frac{h_1}{2} + z \right) \frac{B_1}{\eta_1} + \frac{u_1 - 1}{\eta_1^2} \right] \text{Pe}_1 \frac{\partial \bar{c}_1}{\partial x} + \left( \frac{z^2}{2h_1} + z + \frac{h_1}{3} \right) \frac{\partial c'_1(x, z = 0, t)}{\partial z}, \quad (\text{A22})$$

$$c'_2 = \left[ \left( \frac{z^2}{2} - \frac{h_2^2}{6} + \frac{1}{\eta_2^2} \right) (1 - \bar{u}_2) + \left( \frac{h_2}{2} - z \right) \frac{B_2}{\eta_2} + \frac{u_2 - 1}{\eta_2^2} \right] \text{Pe}_2 \frac{\partial \bar{c}_2}{\partial x} + \left( -\frac{z^2}{2h_2} + z - \frac{h_2}{3} \right) \frac{\partial c'_2(x, z = 0, t)}{\partial z}. \quad (\text{A23})$$

To determine  $\overline{u_1 \partial c'_1 / \partial x}$  and  $\overline{u_2 \partial c'_2 / \partial x}$  in Eqs. (A16) and (A17) and close the mathematical formulation, Eqs. (A22) and (A23) are differentiated with respect to  $x$  to obtain  $\partial c'_1 / \partial x$  and  $\partial c'_2 / \partial x$ :

$$\frac{\partial c'_1}{\partial x} = \left[ \left( \frac{z^2}{2} - \frac{h_1^2}{6} + \frac{1}{\eta_1^2} \right) (1 - \bar{u}_1) - \left( \frac{h_1}{2} + z \right) \frac{B_1}{\eta_1} + \frac{u_1 - 1}{\eta_1^2} \right] \text{Pe}_1 \frac{\partial^2 \bar{c}_1}{\partial x^2} + \left( \frac{z^2}{2h_1} + z + \frac{h_1}{3} \right) \frac{\partial^2 c'_1(x, z = 0, t)}{\partial z \partial x}, \quad (\text{A24})$$

$$\frac{\partial c'_2}{\partial x} = \left[ \left( \frac{z^2}{2} - \frac{h_2^2}{6} + \frac{1}{\eta_2^2} \right) (1 - \bar{u}_2) + \left( \frac{h_2}{2} - z \right) \frac{B_2}{\eta_2} + \frac{u_2 - 1}{\eta_2^2} \right] \text{Pe}_2 \frac{\partial^2 \bar{c}_2}{\partial x^2} + \left( -\frac{z^2}{2h_2} + z - \frac{h_2}{3} \right) \frac{\partial^2 c'_2(x, z = 0, t)}{\partial z \partial x}. \quad (\text{A25})$$

Combination of Eqs. (7) and (8) with Eqs. (A24) and (A25) produces  $\overline{u_1 \partial c'_1 / \partial x}$  and  $\overline{u_2 \partial c'_2 / \partial x}$ :

$$\overline{u_1 \frac{\partial c'_1}{\partial x}} = \frac{1}{h_1} \int_{-h_1}^0 \left( u_1 \frac{\partial c'_1}{\partial x} \right) dz = E_1 \text{Pe}_1 \frac{\partial^2 \bar{c}_1}{\partial x^2} + F_1 \frac{\partial^2 c'_1(x, z = 0, t)}{\partial z \partial x}, \quad (\text{A26})$$

$$\overline{u_2 \frac{\partial c'_2}{\partial x}} = \frac{1}{h_2} \int_0^{h_2} \left( u_2 \frac{\partial c'_2}{\partial x} \right) dz = E_2 \text{Pe}_2 \frac{\partial^2 \bar{c}_2}{\partial x^2} + F_2 \frac{\partial^2 c'_2(x, z = 0, t)}{\partial z \partial x}, \quad (\text{A27})$$

where the constants  $E_1, F_1, E_2$ , and  $F_2$  are defined, respectively, as follows:

$$E_1 = -\frac{(\bar{u}_1 - 1)}{6\eta_1^3 h_1} [(2[\bar{u}_1 - 1]\eta_1 h_1 - 3B_1)\eta_1^2 h_1^2 + 12\eta_1 h_1 \bar{u}_1] + \frac{B_1}{2\eta_1^3 h_1} [\eta_1^2 h_1^2 (\bar{u}_1 - 1) + 2(1 + A_1 - B_1 \eta_1 h_1)] + \frac{1}{2\eta_1^3 h_1} [(\bar{u}_1 - 1)\eta_1 h_1 + (A_1^2 - B_1^2)\eta_1 h_1 + A_1 B_1 + B_1] \quad (\text{A28})$$

$$F_1 = -\frac{1}{6\eta_1^2 h_1} [([\bar{u}_1 - 1]\eta_1 h_1 - 3B_1)\eta_1 h_1 + 6(A_1 - [\bar{u}_1 - 1])], \quad (\text{A29})$$

$$E_2 = -\frac{(\bar{u}_2 - 1)}{6\eta_2^3 h_2} [(2[\bar{u}_2 - 1]\eta_2 h_2 + 3B_2)\eta_2^2 h_2^2 + 12\eta_2 h_2 \bar{u}_2] - \frac{B_2}{2\eta_2^3 h_2} [\eta_2^2 h_2^2 (\bar{u}_2 - 1) + 2(1 + A_2 + B_2 \eta_2 h_2)] + \frac{1}{2\eta_2^3 h_2} [(\bar{u}_2 - 1)\eta_2 h_2 + (A_2^2 - B_2^2)\eta_2 h_2 - A_2 B_2 - B_2], \quad (\text{A30})$$

$$F_2 = \frac{1}{6\eta_2^2 h_2} [([\bar{u}_2 - 1]\eta_2 h_2 + 3B_2)\eta_2 h_2 + 6(A_2 - [\bar{u}_2 - 1])]. \quad (\text{A31})$$

Substitution of Eqs. (A26) and (A27) into Eqs. (A16) and (A17) gives

$$\frac{\partial \bar{c}_1}{\partial t} + \text{Pe}_1 \bar{u}_1 \frac{\partial \bar{c}_1}{\partial x} = (1 - E_1 \text{Pe}_1^2) \frac{\partial^2 \bar{c}_1}{\partial x^2} + \frac{1}{h_1} \frac{\partial c'_1(x, z = 0, t)}{\partial z} - F_1 \text{Pe}_1 \frac{\partial^2 c'_1(x, z = 0, t)}{\partial z \partial x}, \quad (\text{A32})$$

$$D_{1/2} \frac{\partial \bar{c}_2}{\partial t} + \text{Pe}_2 \bar{u}_2 \frac{\partial \bar{c}_2}{\partial x} = (1 - E_2 \text{Pe}_2^2) \frac{\partial^2 \bar{c}_2}{\partial x^2} - \frac{1}{h_2} \frac{\partial c'_2(x, z = 0, t)}{\partial z} - F_2 \text{Pe}_2 \frac{\partial^2 c'_2(x, z = 0, t)}{\partial z \partial x}. \quad (\text{A33})$$

The last two terms on the right-hand side of Eqs. (A32) and (A33) represent the interface between the two strata and produce tensorial dispersion and advection. If both layers have the same permeability ( $k_{1/2} = 1$ ), these terms will disappear. As a result, the tracer transport due to an incompressible single-phase flow of a Newtonian fluid in a porous medium with the nondimensional dispersion coefficient of  $K = 1 - E \text{Pe}^2$  will be achieved. The detailed derivation of the dispersion coefficient in a porous medium can be found in Appendix B.

It is noted that the mathematical formulation developed in this study is valid for  $k_{1/2} \neq 1$ , where the last two terms on the right-hand side of Eqs. (A32) and (A33) are not zero but should be replaced by the appropriate expressions in terms of  $\bar{c}_1$ ,  $\bar{c}_2$ , and their first and second derivatives with respect to  $x$ . To replace  $\partial c'_1(x, z = 0, t)/\partial z$  and  $\partial c'_2(x, z = 0, t)/\partial z$  in Eqs. (A32) and (A33) by the appropriate expressions, first, Eqs. (A22) and (A23) are calculated at  $z = 0$  (where  $u_1(0) = A_1 + 1$  and  $u_2(0) = A_2 + 1$ ) and then they are combined with Eqs. (A13) and (A14):

$$\frac{\partial c'_1(x, z = 0, t)}{\partial z} = J_1 \bar{c}_2 - J_1 \bar{c}_1 + J_1 G_2 \text{Pe}_2 \frac{\partial \bar{c}_2}{\partial x} - J_1 G_1 \text{Pe}_1 \frac{\partial \bar{c}_1}{\partial x}, \quad (\text{A34})$$

$$\frac{\partial c'_2(x, z = 0, t)}{\partial z} = J_2 \bar{c}_2 - J_2 \bar{c}_1 + J_2 G_2 \text{Pe}_2 \frac{\partial \bar{c}_2}{\partial x} - J_2 G_1 \text{Pe}_1 \frac{\partial \bar{c}_1}{\partial x}, \quad (\text{A35})$$

where the constants  $G_1$ ,  $J_1$ ,  $G_2$ , and  $J_2$  are defined, respectively, as follows:

$$G_1 = \left( -\frac{h_1^2}{6} + \frac{1}{\eta_1^2} \right) (1 - \bar{u}_1) - \frac{h_1 B_1}{2 \eta_1} + \frac{A_1}{\eta_1^2}, \quad (\text{A36})$$

$$J_1 = \frac{3}{h_1 + h_2 D_{1/2} \phi_{1/2}}, \quad (\text{A37})$$

$$G_2 = \left( -\frac{h_2^2}{6} + \frac{1}{\eta_2^2} \right) (1 - \bar{u}_2) + \frac{h_2 B_2}{2 \eta_2} + \frac{A_2}{\eta_2^2}, \quad (\text{A38})$$

$$J_2 = \frac{3 D_{1/2} \phi_{1/2}}{h_1 + h_2 D_{1/2} \phi_{1/2}}. \quad (\text{A39})$$

To replace  $\partial^2 c'_1(x, z = 0, t)/\partial z \partial x$  and  $\partial^2 c'_2(x, z = 0, t)/\partial z \partial x$  in Eqs. (A32) and (A33) by the appropriate expressions, Eqs. (A34) and (A35) need to be differentiated with respect to  $x$ :

$$\frac{\partial^2 c'_1(x, z = 0, t)}{\partial z \partial x} = J_1 \frac{\partial \bar{c}_2}{\partial x} - J_1 \frac{\partial \bar{c}_1}{\partial x} + J_1 G_2 \text{Pe}_2 \frac{\partial^2 \bar{c}_2}{\partial x^2} - J_1 G_1 \text{Pe}_1 \frac{\partial^2 \bar{c}_1}{\partial x^2}, \quad (\text{A40})$$

$$\frac{\partial^2 c'_2(x, z = 0, t)}{\partial z \partial x} = J_2 \frac{\partial \bar{c}_2}{\partial x} - J_2 \frac{\partial \bar{c}_1}{\partial x} + J_2 G_2 \text{Pe}_2 \frac{\partial^2 \bar{c}_2}{\partial x^2} - J_2 G_1 \text{Pe}_1 \frac{\partial^2 \bar{c}_1}{\partial x^2}. \quad (\text{A41})$$

Substitution of Eqs. (A34), (A35), (A40), and (A41) into Eqs. (A32) and (A33) leads to the reduced-order models for advection-dispersion tracer transport in stratified porous media (Fig. 1):

$$\begin{aligned} & \frac{\partial \bar{c}_1}{\partial t} + \left( \bar{u}_1 - J_1 F_1 + \frac{1}{h_1} J_1 G_1 \right) \text{Pe}_1 \frac{\partial \bar{c}_1}{\partial x} + \left( J_1 F_1 \text{Pe}_1 - \frac{1}{h_1} J_1 G_2 \text{Pe}_2 \right) \frac{\partial \bar{c}_2}{\partial x} \\ & = \left( 1 - E_1 \text{Pe}_1^2 + J_1 F_1 G_1 \text{Pe}_1^2 \right) \frac{\partial^2 \bar{c}_1}{\partial x^2} - J_1 F_1 G_2 \text{Pe}_1 \text{Pe}_2 \frac{\partial^2 \bar{c}_2}{\partial x^2} + \frac{1}{h_1} J_1 (\bar{c}_2 - \bar{c}_1), \end{aligned} \quad (\text{A42})$$

$$\begin{aligned} & D_{1/2} \frac{\partial \bar{c}_2}{\partial t} + \left( \bar{u}_2 + J_2 F_2 + \frac{1}{h_2} J_2 G_2 \right) \text{Pe}_2 \frac{\partial \bar{c}_2}{\partial x} + \left( -\frac{1}{h_2} J_2 G_1 \text{Pe}_1 - J_2 F_2 \text{Pe}_2 \right) \frac{\partial \bar{c}_1}{\partial x} \\ & = \left( 1 - E_2 \text{Pe}_2^2 - J_2 F_2 G_2 \text{Pe}_2^2 \right) \frac{\partial^2 \bar{c}_2}{\partial x^2} + J_2 F_2 G_1 \text{Pe}_1 \text{Pe}_2 \frac{\partial^2 \bar{c}_1}{\partial x^2} - \frac{1}{h_2} J_2 (\bar{c}_2 - \bar{c}_1). \end{aligned} \quad (\text{A43})$$

Equations (A42) and (A43) are subjected to the following initial and boundary conditions, which are obtained by averaging Eqs. (A10) and (A11), can be solved to result in  $\bar{c}_1$  and  $\bar{c}_2$ :

$$\bar{c}_1(x, t = 0) = \bar{c}_2(x, t = 0) = \delta(x), \quad (\text{A44})$$

$$\bar{c}_1(x \rightarrow \infty, t) = \bar{c}_2(x \rightarrow \infty, t) = 0. \quad (\text{A45})$$

### 3. Special cases

It is valuable to list results for the special cases where the Darcy numbers in porous layers 1 and 2 are either very small or very large.

#### a. Case I: $\text{Da}_1^* \ll 1$ , $\text{Da}_2^* \ll 1$

Suppose the permeabilities of strata 1 and 2 or the ratios of the effective viscosities to the fluid viscosity are very small or the thicknesses of the layers are very large. In that case, the Darcy numbers 1 and 2 will be much smaller than unity ( $\text{Da}_1^* \ll 1$ ,  $\text{Da}_2^* \ll 1$ ). In this special case, the first terms on the left-hand sides of Eqs. (1) and (2),  $\text{Da}_1 d^2 u_1/dz^2$  and  $\text{Da}_2 d^2 u_2/dz^2$ , become negligible and Eqs. (1) and (2) reduce to  $-u_1 + 1 = 0$  and  $-u_2 + 1 = 0$ , respectively, or in other words, the nondimensional velocities in porous media 1 and 2 are unity,  $u_1 = 1$  and  $u_2 = 1$ . This implies that the velocities in both layers are constant and equal to  $\hat{u}_1 = -(k_1/\mu)(d\hat{p}/d\hat{x})$  and  $\hat{u}_2 = -(k_2/\mu)(d\hat{p}/d\hat{x})$ , respectively, which are known as the Darcy equation. Therefore, the third terms on the left-hand sides of Eqs. (A16) and (A17) become zero,  $\overline{u_1 \partial c'_1/\partial x} = \partial c'_1/\partial x = \partial \bar{c}'_1/\partial x = 0$  and  $\overline{u_2 \partial c'_2/\partial x} = \partial c'_2/\partial x = \partial \bar{c}'_2/\partial x = 0$ ; the nondimensional average velocities in strata 1 and 2 become unity,  $\bar{u}_1 = 1$  and  $\bar{u}_2 = 1$ ; and the constants  $E_1$ ,  $F_1$ ,  $G_1$ ,  $E_2$ ,  $F_2$ , and  $G_2$  are all zero. As a result, Eqs. (A42) and (A43) reduce to

$$\frac{\partial \bar{c}_1}{\partial t} + \text{Pe}_1 \frac{\partial \bar{c}_1}{\partial x} = \frac{\partial^2 \bar{c}_1}{\partial x^2} + \frac{1}{h_1} J_1 (\bar{c}_2 - \bar{c}_1), \quad (\text{A46})$$

$$D_{1/2} \frac{\partial \bar{c}_2}{\partial t} + \text{Pe}_2 \frac{\partial \bar{c}_2}{\partial x} = \frac{\partial^2 \bar{c}_2}{\partial x^2} - \frac{1}{h_2} J_2 (\bar{c}_2 - \bar{c}_1). \quad (\text{A47})$$

For this special case, the Taylor or shear dispersion is zero, and the cross-diffusive flux between layers occurs through the source or sink term [which is the last term on the right-hand side of Eqs. (A46) and (A47)]. Therefore, for such a limiting case of Darcy flow in both porous layers, the Taylor dispersion is nonexistent, and the mixing of the injected solute between the two layers is limited to the cross-diffusive flux between layers. The observation suggests that the field scale mixing between layers may not essentially originate from the Taylor dispersion and could be due to the cross-diffusive flux between the layers.

#### b. Case II: $\text{Da}_1^* \gg 1$ , $\text{Da}_2^* \ll 1$

Suppose the permeability of stratum 1 or the ratio of the effective viscosity in porous layer 1 to the fluid viscosity is very large or the thickness of layer 1 is very small. In that case, the Darcy number in stratum 1 will be much larger than unity ( $\text{Da}_1^* \gg 1$ ). In this special case, the second term on the left-hand side of Eq. (1),  $u_1$ , becomes negligible and Eq. (1) reduces to  $\text{Da}_1 d^2 u_1/dz^2 + 1 = 0$ , subject to boundary conditions  $u_1|_{z=-h_1} = 0$  and  $u_1|_{z=0} = 1/\text{Da}_{1/2}$ . This leads to  $u_1(z) = -z^2/2\text{Da}_1 + (1/h_1\text{Da}_{1/2} - h_1/2\text{Da}_1)z + 1/\text{Da}_{1/2}$  as the analytical solution for the nondimensional velocity distribution in porous layer 1. Therefore, the nondimensional average velocity in layer 1 using Eq. (A1) becomes  $\bar{u}_1 = h_1^2/12\text{Da}_1 + 1/2\text{Da}_{1/2}$ .

Suppose the permeability of stratum 2 or the ratio of the effective viscosity in layer 2 to the fluid viscosity is very small or the thickness of layer 2 is very large. In that case, the Darcy number in stratum 2 will be much smaller than unity ( $\text{Da}_2^* \ll 1$ ). In this special case, the first term on the left-hand side of Eq. (2),  $\text{Da}_2 d^2 u_2/dz^2$ , becomes negligible and Eq. (2) reduces to  $-u_2 + 1 = 0$  or, in other words, the nondimensional velocity in porous medium 2 is unity,  $u_2 = 1$ . This implies that the velocity in layer 2 is constant and equal to  $\hat{u}_2 = -(k_2/\mu)(d\hat{p}/d\hat{x})$ , which is known as the Darcy equation. Therefore, the third term on the left-hand side of Eq. (A17) turns to zero,  $\overline{u_2 \partial c'_2/\partial x} = \partial c'_2/\partial x = \partial \bar{c}'_2/\partial x = 0$ , the nondimensional average velocity in stratum 2 becomes unity,  $\bar{u}_2 = 1$ , and the constants  $E_2$ ,  $F_2$ , and  $G_2$  are zero.

If the generalized approach introduced in Sec. II is used, Eqs. (A42) and (A43) become

$$\begin{aligned} \frac{\partial \bar{c}_1}{\partial t} + \left( \bar{u}_1 - J_1 F_1 + \frac{1}{h_1} J_1 G_1 \right) \text{Pe}_1 \frac{\partial \bar{c}_1}{\partial x} + J_1 F_1 \text{Pe}_1 \frac{\partial \bar{c}_2}{\partial x} \\ = (1 - E_1 \text{Pe}_1^2 + J_1 F_1 G_1 \text{Pe}_1^2) \frac{\partial^2 \bar{c}_1}{\partial x^2} + \frac{1}{h_1} J_1 (\bar{c}_2 - \bar{c}_1), \end{aligned} \quad (\text{A48})$$

$$\begin{aligned} D_{1/2} \frac{\partial \bar{c}_2}{\partial t} + \text{Pe}_2 \frac{\partial \bar{c}_2}{\partial x} + \left( -\frac{1}{h_2} J_2 G_1 \text{Pe}_1 \right) \frac{\partial \bar{c}_1}{\partial x} \\ = \frac{\partial^2 \bar{c}_2}{\partial x^2} - \frac{1}{h_2} J_2 (\bar{c}_2 - \bar{c}_1), \end{aligned} \quad (\text{A49})$$

where the constants  $J_1$  and  $J_2$  are defined by Eqs. (A37) and (A39), respectively, and the constants  $E_1$ ,  $F_1$ , and  $G_1$  are defined, respectively, as follows:

$$E_1 = -\frac{h_1^6}{30240\text{Da}_1^2} - \frac{h_1^2}{120\text{Da}_{1/2}^2}, \quad (\text{A50})$$

$$F_1 = \frac{h_1}{24\text{Da}_{1/2}} - \frac{h_1^3}{720\text{Da}_1}, \quad (\text{A51})$$

$$G_1 = \frac{h_1^4}{720\text{Da}_1} - \frac{h_1^2}{24\text{Da}_{1/2}}. \quad (\text{A52})$$

#### c. Case III: $\text{Da}_1^* \ll 1$ , $\text{Da}_2^* \gg 1$

If the permeability of layer 1 or the ratio of the effective viscosity in layer 1 to the fluid viscosity is very small or the thickness of layer 1 is very large, it results in  $\text{Da}_1^* \ll 1$ . In this special case, the first term on the left-hand side of Eq. (1),  $\text{Da}_1 d^2 u_1/dz^2$ , becomes negligible and Eq. (1) reduces to  $-u_1 + 1 = 0$  or, in other words, the nondimensional velocity in layer 1 is unity,  $u_1 = 1$ . This implies that the velocity in layer 1 is constant and equal to  $\hat{u}_1 = -(k_1/\mu)(d\hat{p}/d\hat{x})$ . Therefore, the third term on the left-hand side of Eq. (A16) turns to zero,  $\overline{u_1 \partial c'_1/\partial x} = \partial c'_1/\partial x = \partial \bar{c}'_1/\partial x = 0$ ; the nondimensional average velocity in layer 1 becomes unity,  $\bar{u}_1 = 1$ ; and the constants  $E_1$ ,  $F_1$ , and  $G_1$  are zero.

If the permeability of layer 2 or the ratio of the effective viscosity in layer 2 to the fluid viscosity is very large or the thickness of layer 2 is very small, it results in  $\text{Da}_2^* \gg 1$ . In this special case, the second term on the left-hand side of Eq. (2),  $u_2$ , can be ignored and Eq. (2) reduces to  $\text{Da}_2 d^2 u_2/dz^2 + 1 = 0$ . Subject to boundary conditions  $u_2|_{z=0} = \text{Da}_{1/2}$  and

$u_2|_{z=h_2} = 0$ , it will lead to  $u_2(z) = -z^2/2\text{Da}_2 + (h_2/2\text{Da}_2 - \text{Da}_{1/2}/h_2)z + \text{Da}_{1/2}$ . Therefore, the nondimensional average

velocity in layer 2 using Eq. (A2) becomes  $\bar{u}_2 = h_2^2/12\text{Da}_2 + \text{Da}_{1/2}/2$ .

If the generalized approach introduced in Sec. II is followed, Eqs. (A42) and (A43) will become

$$\frac{\partial \bar{c}_1}{\partial t} + \text{Pe}_1 \frac{\partial \bar{c}_1}{\partial x} + \left( -\frac{1}{h_1} J_1 G_2 \text{Pe}_2 \right) \frac{\partial \bar{c}_2}{\partial x} = \frac{\partial^2 \bar{c}_1}{\partial x^2} + \frac{1}{h_1} J_1 (\bar{c}_2 - \bar{c}_1), \quad (\text{A53})$$

$$D_{1/2} \frac{\partial \bar{c}_2}{\partial t} + \left( \bar{u}_2 + J_2 F_2 + \frac{1}{h_2} J_2 G_2 \right) \text{Pe}_2 \frac{\partial \bar{c}_2}{\partial x} - J_2 F_2 \text{Pe}_2 \frac{\partial \bar{c}_1}{\partial x} = (1 - E_2 \text{Pe}_2^2 - J_2 F_2 G_2 \text{Pe}_2^2) \frac{\partial^2 \bar{c}_2}{\partial x^2} - \frac{1}{h_2} J_2 (\bar{c}_2 - \bar{c}_1), \quad (\text{A54})$$

where the constants  $J_1$  and  $J_2$  are defined by Eqs. (A37) and (A39), respectively, and the constants  $E_2$ ,  $F_2$ , and  $G_2$  are defined, respectively, as follows:

$$E_2 = -\frac{h_2^6}{30240\text{Da}_2^2} - \frac{\text{Da}_{1/2}^2 h_2^2}{120}, \quad (\text{A55})$$

$$F_2 = \frac{h_2^3}{720\text{Da}_2} - \frac{\text{Da}_{1/2} h_2}{24}, \quad (\text{A56})$$

$$G_2 = \frac{h_2^4}{720\text{Da}_2} - \frac{\text{Da}_{1/2} h_2^2}{24}. \quad (\text{A57})$$

#### d. Case IV: $\text{Da}_1^* \gg 1$ , $\text{Da}_2^* \gg 1$

If the permeabilities or the ratios of the effective viscosities of both layers are very large or the thicknesses of layers are very small, it results in  $\text{Da}_1^* \gg 1$ ,  $\text{Da}_2^* \gg 1$ . In this special case, the second terms on the left-hand sides of Eqs. (1) and (2),  $u_1$  and  $u_2$ , become negligible and Eqs. (1) and (2) reduce to  $\text{Da}_1 d^2 u_1/dz^2 + 1 = 0$  and  $\text{Da}_2 d^2 u_2/dz^2 + 1 = 0$ , respectively. Subject to Eqs. (3)–(6), they will lead to  $u_1(z) = -z^2/2\text{Da}_1 + (h_2 - h_1)z/2\text{Da}_1 + h_1 h_2/2\text{Da}_1$  and  $u_2(z) = -z^2/2\text{Da}_2 + (h_2 - h_1)z/2\text{Da}_2 + h_1 h_2/2\text{Da}_2$  as the analytical solutions for the nondimensional velocity distributions. Therefore, the nondimensional average velocities using Eqs. (A1) and (A2) become  $\bar{u}_1 = h_1^2/12\text{Da}_1 + h_1 h_2/4\text{Da}_1$  and  $\bar{u}_2 = h_2^2/12\text{Da}_2 + h_1 h_2/4\text{Da}_2$ , respectively. Following the generalized approach introduced in Sec. II, Eqs. (A42) and (A43) will become

$$\begin{aligned} \frac{\partial \bar{c}_1}{\partial t} + \left( \bar{u}_1 - J_1 F_1 + \frac{1}{h_1} J_1 G_1 \right) \text{Pe}_1 \frac{\partial \bar{c}_1}{\partial x} + \left( J_1 F_1 \text{Pe}_1 - \frac{1}{h_1} J_1 G_2 \text{Pe}_2 \right) \frac{\partial \bar{c}_2}{\partial x} \\ = (1 - E_1 \text{Pe}_1^2 + J_1 F_1 G_1 \text{Pe}_1^2) \frac{\partial^2 \bar{c}_1}{\partial x^2} - J_1 F_1 G_2 \text{Pe}_1 \text{Pe}_2 \frac{\partial^2 \bar{c}_2}{\partial x^2} + \frac{1}{h_1} J_1 (\bar{c}_2 - \bar{c}_1), \end{aligned} \quad (\text{A58})$$

$$\begin{aligned} D_{1/2} \frac{\partial \bar{c}_2}{\partial t} + \left( \bar{u}_2 + J_2 F_2 + \frac{1}{h_2} J_2 G_2 \right) \text{Pe}_2 \frac{\partial \bar{c}_2}{\partial x} + \left( -\frac{1}{h_2} J_2 G_1 \text{Pe}_1 - J_2 F_2 \text{Pe}_2 \right) \frac{\partial \bar{c}_1}{\partial x} \\ = (1 - E_2 \text{Pe}_2^2 - J_2 F_2 G_2 \text{Pe}_2^2) \frac{\partial^2 \bar{c}_2}{\partial x^2} + J_2 F_2 G_1 \text{Pe}_1 \text{Pe}_2 \frac{\partial^2 \bar{c}_1}{\partial x^2} - \frac{1}{h_2} J_2 (\bar{c}_2 - \bar{c}_1), \end{aligned} \quad (\text{A59})$$

where the constants  $J_1$  and  $J_2$  are defined by Eqs. (A37) and (A39), respectively, and the constants  $E_1$ ,  $F_1$ ,  $G_1$ ,  $E_2$ ,  $F_2$ , and  $G_2$  are defined, respectively, as follows:

$$E_1 = -\frac{h_1^3}{720\text{Da}_1^2} \left( \frac{3h_1^3}{28} - h_1^2 h_2 - \frac{9}{4} h_1 h_2^2 - \text{Da}_1 \bar{u}_1 h_1 + 15\text{Da}_1 \bar{u}_1 h_2 \right), \quad (\text{A60})$$

$$F_1 = -\frac{h_1^2}{720\text{Da}_1} (h_1 - 15h_2), \quad (\text{A61})$$

$$G_1 = -\frac{h_1^2}{\text{Da}_1} \left( -\frac{7}{240} h_1^2 - \frac{1}{16} h_1 h_2 + \frac{1}{3} \bar{u}_1 \text{Da}_1 \right), \quad (\text{A62})$$

$$E_2 = -\frac{h_2^3}{720\text{Da}_2^2} \left( \frac{3h_2^3}{28} - h_1 h_2^2 - \frac{9}{4} h_1^2 h_2 - \text{Da}_2 \bar{u}_2 h_2 + 15\text{Da}_2 \bar{u}_2 h_1 \right), \quad (\text{A63})$$

$$F_2 = -\frac{h_2^2}{720\text{Da}_2} (15h_1 - h_2), \quad (\text{A64})$$

$$G_2 = -\frac{h_2^2}{\text{Da}_2} \left( -\frac{7}{240} h_2^2 - \frac{1}{16} h_1 h_2 + \frac{1}{3} \bar{u}_2 \text{Da}_2 \right). \quad (\text{A65})$$

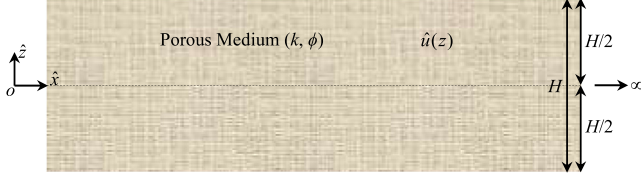


FIG. 9. The physical model for tracer transport in the porous medium.

## APPENDIX B: DISPERSION COEFFICIENT IN A SINGLE-LAYER POROUS MEDIUM AND SPECIAL CASES

### 1. Physical model and assumptions

Figure 9 shows the tracer transport in a porous medium of thickness  $H$  and length  $\infty$ . The porous medium's inlet and center are the origins of the longitudinal and transversal directions (or the  $\hat{x}$  and  $\hat{z}$  directions), respectively. Therefore, the porous medium occupies the domain  $\hat{z} \in [-H/2, H/2]$ . The physical properties of the porous medium such as permeability and porosity, and the physical properties of fluid, such as density and viscosity, remain constant. The permeability and porosity of the porous medium are  $k$  and  $\phi$ , respectively. The fluid is Newtonian incompressible single-phase and flows in the porous medium under a fully developed laminar condition with the velocity distribution  $\hat{u}(z)$ .

### 2. Derivation of velocity distribution

The fully developed Stokes flow in the porous medium can be described by the Darcy-Brinkman equation, which is the second-order linear ordinary differential equation, in nondimensional form as follows:

$$\text{Da} \frac{d^2 u}{dz^2} - u + 1 = 0, \quad z \in (-1/2, 1/2), \quad (\text{B1})$$

where  $u = \hat{u} / -[(k/\mu)(d\hat{p}/d\hat{x})]$ ,  $z = \hat{z}/H$ , and  $\text{Da} = (\mu_e/\mu)(k/H^2)$ , in which  $\hat{u}$  is the velocity in the porous medium,  $u$  is the nondimensional velocity,  $\mu$  is the fluid viscosity,  $\mu_e$  is the effective viscosity in the porous medium,  $\hat{p}$  is the pressure,  $d\hat{p}/d\hat{x}$  is the pressure gradient (which is constant and drives the flow in the longitudinal direction),  $z$  is the nondimensional transversal coordinate, and  $\text{Da}$  is the Darcy number.

Equation (B1) is subject to the no-slip condition at the bottom ( $z = -1/2$ ) and top ( $z = 1/2$ ):

$$u|_{z=-1/2} = 0, \quad (\text{B2})$$

$$u|_{z=1/2} = 0. \quad (\text{B3})$$

The following analytical solution for the nondimensional velocity distribution in the porous medium can be derived by solving Eq. (B1) subject to Eqs. (B2) and (B3):

$$u(z) = A \cosh(\eta z) + 1, \quad z \in [-1/2, 1/2], \quad (\text{B4})$$

where the constant  $A$  is defined as follows:

$$A = -\text{sech}\lambda, \quad (\text{B5})$$

where  $\lambda = \eta/2 = H/2\sqrt{k}$ .

### 3. Governing equation for advection-diffusion tracer transport

The tracer transport in the porous medium can be described by the advection-diffusion equation, which is the second-order nonlinear partial differential equation, in nondimensional form as follows:

$$\frac{\partial c}{\partial t} + \text{Pe}u \frac{\partial c}{\partial x} = \frac{\partial^2 c}{\partial x^2} + \frac{\partial^2 c}{\partial z^2},$$

$$x \in (0, \infty), \quad z \in (-1/2, 1/2), \quad t > 0, \quad (\text{B6})$$

where  $c = \hat{c}/c^*$ ,  $x = \hat{x}/H$ ,  $t = D\hat{t}/H^2$ , and  $\text{Pe} = -[(k/\mu)(d\hat{p}/d\hat{x})]H/D\phi$ , in which  $\hat{c}$  is the tracer concentration,  $c$  is the nondimensional tracer concentration,  $c^*$  is the reference tracer concentration,  $x$  is the nondimensional longitudinal coordinate,  $\hat{t}$  is the time,  $t$  is the nondimensional time,  $D$  is the molecular diffusion coefficient, and  $\text{Pe}$  is the Péclet number for fluid flow in the porous medium.

Equation (B6) is subject to the instantaneous injection of the tracer at  $t = 0$  (as a pulse) at the inlet of the porous medium ( $x = 0$ ), zero tracer concentration at infinite distance from the inlet ( $x \rightarrow \infty$ ), and no-mass flux at the bottom ( $z = -1/2$ ) and top ( $z = 1/2$ ) of the porous medium:

$$c[x \in (0, \infty), z \in (-1/2, 1/2), t = 0] = \delta(x), \quad (\text{B7})$$

$$c[x \rightarrow \infty, z \in (-1/2, 1/2), t > 0] = 0, \quad (\text{B8})$$

$$\frac{\partial c[x \in (0, \infty), z = -1/2, t > 0]}{\partial z} = 0, \quad (\text{B9})$$

$$\frac{\partial c[x \in (0, \infty), z = 1/2, t > 0]}{\partial z} = 0. \quad (\text{B10})$$

### 4. Reynolds decomposition and averaging methods

The Reynolds decomposition, which is a technique to split the average and fluctuation components of a variable [33], can be used to write the nondimensional velocity and tracer concentration, respectively, as follows:

$$u(z) = \bar{u} + u'(z) = \int_{-1/2}^{1/2} u dz + u'(z), \quad (\text{B11})$$

$$c(x, z, t) = \bar{c}(x, t) + c'(x, z, t) = \int_{-1/2}^{1/2} c dz + c'(x, z, t), \quad (\text{B12})$$

where  $\bar{u}$  and  $\bar{c}$  are the nondimensional average velocity and tracer concentration, respectively, and  $u'$  and  $c'$  are the fluctuation components. The averages of the fluctuation components are zero based on the Reynolds decomposition [33]:

$$\int_{-1/2}^{1/2} u' dz = \int_{-1/2}^{1/2} c' dz = 0. \quad (\text{B13})$$

The following expression can be derived for the nondimensional average velocity using Eqs. (B4) and (B11):

$$\bar{u} = \frac{2A}{\eta} \sinh(\eta/2) + 1. \quad (\text{B14})$$

### 5. Derivation of reduced-order model for advection-dispersion tracer transport

If  $c$  from Eq. (B12) is substituted into Eqs. (B6)–(B10), the following equations can be derived:

$$\frac{\partial \bar{c}}{\partial t} + \frac{\partial c'}{\partial t} + \text{Pe}u \frac{\partial \bar{c}}{\partial x} + \text{Pe}u \frac{\partial c'}{\partial x} = \frac{\partial^2 \bar{c}}{\partial x^2} + \frac{\partial^2 c'}{\partial x^2} + \frac{\partial^2 c'}{\partial z^2}, \quad (\text{B15})$$

$$\bar{c}(x, t = 0) + c'(x, z, t = 0) = \delta(x), \quad (\text{B16})$$

$$\bar{c}(x \rightarrow \infty, t) + c'(x \rightarrow \infty, z, t) = 0, \quad (\text{B17})$$

$$\frac{\partial c'(x, z = -1/2, t)}{\partial z} = 0, \quad (\text{B18})$$

$$\frac{\partial c'(x, z = 1/2, t)}{\partial z} = 0. \quad (\text{B19})$$

Averaging Eq. (B15) with the aid of Eqs. (B13), (B18), and (B19) results in

$$\frac{\partial \bar{c}}{\partial t} + \text{Pe}\bar{u} \frac{\partial \bar{c}}{\partial x} + \text{Pe}u \frac{\partial c'}{\partial x} = \frac{\partial^2 \bar{c}}{\partial x^2}. \quad (\text{B20})$$

Subtraction of Eq. (B20) from Eq. (B15) leads to

$$\frac{\partial c'}{\partial t} + \text{Pe}(u - \bar{u}) \frac{\partial \bar{c}}{\partial x} + \text{Pe}u \frac{\partial c'}{\partial x} - \text{Pe}u \frac{\partial c'}{\partial x} = \frac{\partial^2 c'}{\partial x^2} + \frac{\partial^2 c'}{\partial z^2}. \quad (\text{B21})$$

The exact Eq. (B21) is now exposed to three following assumptions adopted by Taylor [1] and Fischer *et al.* [4] on the tracer transport.

(i)  $\partial c'/\partial t \approx 0$  indicates a quasisteady state condition, which can be considered after passing sufficient time from the tracer introduction at the inlet of the porous medium if the fluctuation component in the transversal direction in the porous medium is smoothed out by the transversal diffusion. This infers that  $\bar{c} \gg c'$ , where the average tracer concentration in the porous medium becomes much larger than the fluctuation component. Therefore, the fluctuation component in the transversal direction in the porous medium is negligible. For the timescale in the order of magnitudes of the diffusion time across the porous medium, which is  $H^2/D$ , this assumption can be taken into consideration.

(ii)  $c'$ , which is the fluctuation component of the tracer concentration, varies slowly. This infers that  $\text{Pe}u \partial c'/\partial x \approx \text{Pe}u \partial \bar{c}/\partial x$ .

(iii)  $\text{Pe}(u - \bar{u}) \partial \bar{c}/\partial x \gg \partial^2 c'/\partial x^2$  shows that the longitudinal diffusion can be ignored compared to the longitudinal advection. Therefore, the impact of the longitudinal diffusion is not considerable, and the tracer transport is mainly controlled by the longitudinal advection and the transversal diffusion.

If assumptions (i)–(iii) are used, Eq. (B21) will reduce to

$$\text{Pe}(u - \bar{u}) \frac{\partial \bar{c}}{\partial x} = \frac{\partial^2 c'}{\partial z^2}. \quad (\text{B22})$$

If Eq. (B22) is integrated twice with respect to  $z$  and the resulting expression is subject to Eqs. (B13), (B18), and (B19) to find the constants of integrations,  $c'$  will be derived as

follows:

$$c' = \left[ (1 - \bar{u}) \frac{z^2}{2} - \frac{1 - u}{\eta^2} - \left( \frac{1}{24} - \frac{1}{\eta^2} \right) (1 - \bar{u}) \right] \text{Pe} \frac{\partial \bar{c}}{\partial x}. \quad (\text{B23})$$

To determine  $\overline{u \partial c'/\partial x}$  in Eq. (B20) and finalize the mathematical formulation, Eq. (B23) is differentiated with respect to  $x$  to obtain  $\partial c'/\partial x$ :

$$\frac{\partial c'}{\partial x} = \left[ (1 - \bar{u}) \frac{z^2}{2} - \frac{1 - u}{\eta^2} - \left( \frac{1}{24} - \frac{1}{\eta^2} \right) (1 - \bar{u}) \right] \text{Pe} \frac{\partial^2 \bar{c}}{\partial x^2}. \quad (\text{B24})$$

Combination of Eq. (B4) with Eq. (B24) produces  $\overline{u \partial c'/\partial x}$ :

$$\overline{u \frac{\partial c'}{\partial x}} = \int_{-1/2}^{1/2} \left( u \frac{\partial c'}{\partial x} \right) dz = E \text{Pe} \frac{\partial^2 \bar{c}}{\partial x^2}, \quad (\text{B25})$$

where the constant  $E$  is defined as follows:

$$E = -\frac{A^2}{3\eta^4} \left[ (\eta^2 + 24) \cosh^2 \left( \frac{\eta}{2} \right) - 9\eta \cosh \left( \frac{\eta}{2} \right) \sinh \left( \frac{\eta}{2} \right) - \frac{5\eta^2}{2} - 24 \right] - \frac{A^2}{3\eta^4} \left[ \frac{(\eta^2 + 24)}{A^2} + \frac{9\eta^2}{2A^2} (\bar{u} - 1) - \frac{5\eta^2}{2} - 24 \right]. \quad (\text{B26})$$

Substitution of Eq. (B25) into Eq. (B20) leads to the reduced-order model for advection-dispersion tracer transport in the porous medium (Fig. 9):

$$\frac{\partial \bar{c}}{\partial t} + \text{Pe}\bar{u} \frac{\partial \bar{c}}{\partial x} = (1 - E \text{Pe}^2) \frac{\partial^2 \bar{c}}{\partial x^2}, \quad (\text{B27})$$

where  $K = 1 - E \text{Pe}^2$  is the nondimensional dispersion coefficient in the porous medium.

Equation (B27) subject to the following initial and boundary conditions, which are obtained by averaging Eqs. (B16) and (B17), can be solved to result in  $c$ :

$$\bar{c}(x, t = 0) = \delta(x), \quad (\text{B28})$$

$$\bar{c}(x \rightarrow \infty, t) = 0. \quad (\text{B29})$$

### 6. Special cases

It is useful to list special results for the cases of very small and very large Darcy numbers.

Suppose the permeability of the porous medium or the ratio of the effective viscosity in the porous medium to the fluid viscosity is very small or the thickness of the porous medium is very large. In that case, the Darcy number in the porous medium will be much smaller than unity ( $\text{Da} \ll 1$ ). In this special case, the first term on the left-hand side of Eq. (B1),  $\text{Da} d^2 u/dz^2$ , becomes negligible and Eq. (B1) reduces to  $-u + 1 = 0$  or, in other words, the nondimensional velocity in the porous medium is unity,  $u = 1$ . This implies that the velocity in the porous medium is constant and equal to  $\hat{u} = -(k/\mu)(d\hat{p}/d\hat{x})$ , which is known as the Darcy equation. Therefore, the third term on the left-hand side of Eq. (B20)

becomes zero,  $\overline{u\partial c'/\partial x} = \overline{\partial c'/\partial x} = \partial \overline{c'}/\partial x = 0$ ; the nondimensional average velocity in the porous medium becomes unity,  $\overline{u} = 1$ ; and the constant  $E$  is zero. As a result, Eq. (B27) reduces to  $\partial \overline{c'}/\partial t + \text{Pe}\partial \overline{c'}/\partial x = \partial^2 \overline{c'}/\partial x^2$ , which indicates that the Taylor [1] or shear dispersion is zero and  $K = 1$ .

If the permeability of the porous medium or the ratio of the effective viscosity in the porous medium to the fluid viscosity is very large or the thickness of the porous medium is very small, the Darcy number in porous medium will be much larger than unity ( $\text{Da} \gg 1$ ). In this special case, the second

term on the left-hand side of Eq. (B1),  $u$ , becomes ignorable and Eq. (B1) reduces to  $\text{Da}d^2u/dz^2 + 1 = 0$ . Subject to Eqs. (B2) and (B3), it will lead to  $u(z) = (1/2\text{Da})(1/4 - z^2)$  as the analytical solution for the nondimensional velocity distribution in the porous medium. Therefore, the nondimensional average velocity in the porous medium using Eq. (B11) becomes  $\overline{u} = 1/12\text{Da}$ . If the mathematical approach applied in this study is used, the nondimensional dispersion coefficient of  $K = 1 + (1/144\text{Da}^2)(\text{Pe}^2/210)$  will be derived.

- 
- [1] G. Taylor, Dispersion of soluble matter in solvent flowing slowly through a tube, *Proc. R. Soc. London, Ser. A* **219**, 186 (1953).
- [2] B. Berkowitz and J. Zhou, Reactive solute transport in a single fracture, *Water Resour. Res.* **32**, 901 (1996).
- [3] M. Dejam, Advective-diffusive-reactive solute transport due to non-Newtonian fluid flows in a fracture surrounded by a tight porous medium, *Int. J. Heat Mass Transfer* **128**, 1307 (2019).
- [4] H. B. Fischer, E. J. List, R. C. Y. Koh, J. Imberger, and N. H. Brooks, *Mixing in Inland and Coastal Waters* (Academic Press, San Diego, CA, 1979).
- [5] M. Dejam, H. Hassanzadeh, and Z. Chen, Shear dispersion in combined pressure-driven and electro-osmotic flows in a capillary tube with a porous wall, *Am. Inst. Chem. Eng. J.* **61**, 3981 (2015).
- [6] M. Dejam, Derivation of dispersion coefficient in an electro-osmotic flow of a viscoelastic fluid through a porous-walled microchannel, *Chem Eng. Sci.* **204**, 298 (2019).
- [7] R. Lima, T. Ishikawa, Y. Imai, M. Takeda, S. Wada, and T. Yamaguchi, Radial dispersion of red blood cells in blood flowing through glass capillaries: The role of hematocrit and geometry, *J. Biomech.* **41**, 2188 (2008).
- [8] L. W. Lake and G. J. Hirasaki, Taylor's dispersion in stratified porous media, *Soc. Pet. Eng. J.* **21**, 459 (1981).
- [9] N. Garapati, J. B. Randolph, J. L. Valencia Jr., and M. O. Saar, CO<sub>2</sub>-plume geothermal (CPG) heat extraction in multi-layered geologic reservoirs, *Energy Procedia* **63**, 7631 (2014).
- [10] H. Hassanzadeh, M. Pooladi-Darvish, and D. W. Keith, The effect of natural flow of aquifers and associated dispersion on the onset of buoyancy-driven convection in a saturated porous medium, *Am. Inst. Chem. Eng. J.* **55**, 475 (2009).
- [11] H. Emami Meybodi and H. Hassanzadeh, Hydrodynamic dispersion in steady buoyancy-driven geological flows, *Water Resour. Res.* **47**(12), W12504 (2011).
- [12] L. Paterson, The implications of fingering in underground hydrogen storage, *Int. J. Hydrogen Energy* **8**, 53 (1983).
- [13] L. Dassi, Investigation by multivariate analysis of groundwater composition in a multilayer aquifer system from North Africa: A multi-tracer approach, *J. Appl. Geochem.* **26**, 1386 (2011).
- [14] Z. Wu, G. Q. Chen, and L. Zeng, Environmental dispersion in a two-zone wetland, *Ecol. Modell.* **222**, 456 (2011).
- [15] L. Krasemann, A. Toutianoush, and B. Tieke, Self-assembled polyelectrolyte multilayer membranes with highly improved pervaporation separation of ethanol/water mixtures, *J. Membr. Sci.* **181**, 221 (2001).
- [16] X. Zhang, T. Liang, and Q. Ma, Layer-by-layer assembled nano-drug delivery systems for cancer treatment, *Drug Deliv.* **28**, 655 (2021).
- [17] R. Aris, On the dispersion of a solute by diffusion, convection and exchange between phases, *Proc. R. Soc. London, Ser. A* **252**, 538 (1959).
- [18] C.-O. Ng, A note on the Aris dispersion in a tube with phase exchange and reaction, *Int. J. Eng. Sci.* **38**, 1639 (2000).
- [19] Z. Wu and G. Q. Chen, Dispersion in a two-zone packed tube: An extended Taylor's analysis, *Int. J. Eng. Sci.* **50**, 113 (2012).
- [20] I. M. Griffiths, P. D. Howell, and R. J. Shipley, Control and optimization of solute transport in a thin porous tube, *Phys. Fluids* **25**, 033101 (2013).
- [21] G. S. Beavers and D. D. Joseph, Boundary conditions at a naturally permeable wall, *J. Fluid Mech.* **30**, 197 (1967).
- [22] B. Ling, A. M. Tartakovsky, and I. Battiato, Dispersion controlled by permeable surfaces: Surface properties and scaling, *J. Fluid Mech.* **801**, 13 (2016).
- [23] B. Ling, C. B. Rizzo, I. Battiato, and F. P. J. de Barros, Macroscale transport in channel-matrix systems via integral transforms, *Phys. Rev. Fluids* **6**, 044501 (2021).
- [24] M. Dejam, H. Hassanzadeh, and Z. Chen, Shear dispersion in a fracture with porous walls, *Adv. Water Resour.* **74**, 14 (2014).
- [25] Z. Kou and M. Dejam, Dispersion due to combined pressure-driven and electro-osmotic flows in a channel surrounded by a permeable porous medium, *Phys. Fluids* **31**, 056603 (2019).
- [26] M. Dejam and H. Hassanzadeh, Dispersion tensor in a two-phase flow in a slit, *Phys. Fluids* **33**, 103612 (2021).
- [27] H. Emami Meybodi and H. Hassanzadeh, Mixing induced by buoyancy-driven flows in porous media, *Am. Inst. Chem. Eng. J.* **59**, 1378 (2013).
- [28] H. L. Toor, Diffusion in three-component gas mixtures, *Am. Inst. Chem. Eng. J.* **3**, 198 (1957).
- [29] R. Taylor and R. Krishna, *Multicomponent Mass Transfer* (John Wiley, New York, 1993).
- [30] R. Krishna, Uphill diffusion in multicomponent mixtures, *Chem. Soc. Rev.* **44**, 2812 (2015).
- [31] A. Lauerer, T. Binder, C. Chmelik, E. Miersemann, J. Haase, D. M. Ruthven, and J. Kärger, Uphill diffusion and overshooting in the adsorption of binary mixtures in nanoporous solids, *Nat. Commun.* **6**, 7697 (2015).
- [32] K. Aziz and A. Settari, *Petroleum Reservoir Simulation* (Elsevier Applied Science Publishers, London, 1979).

- [33] R. B. Bird, W. E. Stewart, and E. N. Lightfoot, *Transport Phenomena* (John Wiley, New York, 1960).
- [34] V. Ananthakrishnan, W. N. Gill, and A. J. Barduhn, Laminar dispersion in capillaries: Part I. Mathematical analysis, *AIChE J.* **11**, 1063 (1965).
- [35] L. W. Gelhar and C. L. Axness, Three-dimensional stochastic analysis of macrodispersion in aquifers, *Water Resour. Res.* **19**, 161 (1983).
- [36] J. Bear, *Dynamics of Fluids in Porous Media* (Dover Publications, New York, 1988).